IOSUD – ”DUNĂREA DE JOS” UNIVERSITY OF GALAȚI

Doctoral School of Mechanical and Industrial Engineering

DOCTORAL THESIS

ABSTRACT

RESEARCH AND CONTRIBUTIONS ON DIAGNOSING THE TECHNICAL CONDITION OF VEHICLES

PhD. student,
Eng. Mihai GINGĂRAȘU

Scientific coordinator,
Prof. dr. eng. Elena MEREUȚĂ

Series I6: Mechanical Engineering No. 55

GALAȚI

2021

IOSUD – ”DUNĂREA DE JOS” UNIVERSITY OF GALAȚI

Doctoral School of Mechanical and Industrial Engineering

DOCTORAL THESIS

ABSTRACT

RESEARCH AND CONTRIBUTIONS ON DIAGNOSING THE TECHNICAL CONDITION OF VEHICLES

PhD. student,
Eng. Mihai GINGĂRAȘU

Chairman of the Scientific Committee	**Prof. dr. eng. Eugen Victor Cristian RUSU** ”Dunărea de Jos” University of Galați
Scientific coordinator	**Prof. dr. eng. Elena MEREUȚĂ** ”Dunărea de Jos” University of Galați
Scientific reviewers	**Prof. dr. eng. Daniel CONDURACHE** ”Gheorghe Asachi” Technical University of Iași **Prof. dr. eng. Ioan Călin ROȘCA** ”Transilvania” University of Brașov **Prof. dr. eng. Daniela TARNIȚĂ** University of Craiova

Series I6: Mechanical Engineering No. 55

GALAȚI

2021

CONTENTS

KEYWORDS: diagnostics, steering system, tie rod end, spherical joint, vibrations.

CHAPTER 1
INTRODUCTION

1.1 Motivation of choosing the topic and objectives of the doctoral thesis

In the current context of the intensification, both at national and international level, of road transport, the need for the safe development of road traffic is a key desideratum of the operation of vehicles [1], [2].

This doctoral thesis aims to diagnose the wear of spherical joints produced at the tie rod end of the steering systems. The consequences of these defects are the change in the geometry of the steering system, the loss of stability of the vehicle, both in corners and in straight running, difficulties in entering the controlled trajectory, accelerated wear of tires or other components of the steering system and even risk of road accident [2], [3], [4].

The purpose of the doctoral thesis is to develop a method for diagnosing during running the wear of spherical joints of the steering system, having as a starting point the symptoms that an experienced driver perceives in running (sounds, vibrations, abnormal shocks). Early detection of such malfunctions would play an important role in increasing road comfort and safety and reducing vehicle maintenance costs [3], [5], [6], [7].

In order to achieve the goal of the doctoral thesis, the following objectives were established:

a) analysis of the current state of research on diagnosing the technical condition of vehicles;

b) analysis of the vehicle-driveway interaction and the role of the human factor in this interaction;

c) the analysis of the way of performing the technical condition inspection of the steering systems, respecting the the national, the European and the international norms;

d) identification of the symptoms attesting the production of wear of the spherical joints, the appearance of shocks in the worn joints and establishing the response to the shocks in these joints;

e) modeling with finite elements of the dynamic response of the tie rod – tie rod end assembly of the steering system, wich has in its structure the spherical joint;

f) analysis of the shock response of the assembly with or without defect having different values in the spherical joint, by modeling with finite elements, using the Ansys program;

g) making experimental recordings on the test bench, in order to establish the response of the analyzed system to the shock;

h) making experimental recordings during running, to establish the response of the analyzed system to shock, in different running conditions and depending on the technical condition of the spherical joint;

i) elaboration of a mathematical model based on the input-output data recorded at the running tests and its validation;

j) the analysis of the experimental data and the establishment of their quantities and values that attest the occurrence of defects at the spherical joints of the steering system.

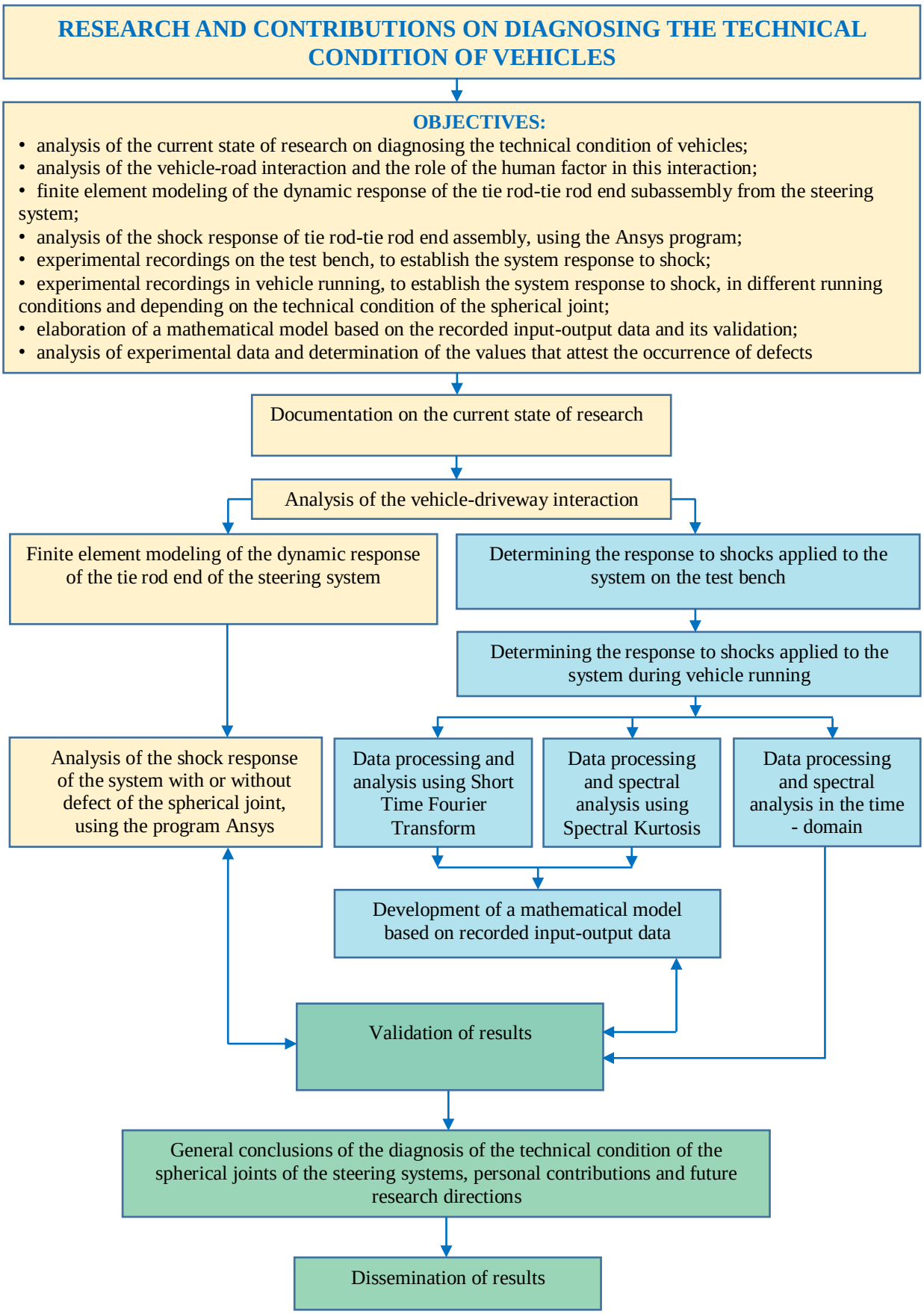

Figure 1. 1 Thesis diagram

1.2 Considerations regarding the vehicle evolution and driving

1.2.1 Presentation of the vehicles evolution

The development of the vehicle was fast, both in terms of technology and design, being marked by various social and cultural developments, to reach the current level. Electronic control systems are more and more used in the automotive industry to provide comfort and safety to equipment, drivers and passengers, with increased levels of authorization and control. An increasing trend is to assist the driver in maintaining a control as secure as possible on the movement of the vehicle in various situations, such as congested traffic conditions, various weather conditions, different technical conditions of vehicle equipment and different levels of driver qualification [8], [9], [10].

1.2.2 Driver-vehicle-environment system. Components, interactions, interconnections

The need to safety operate the vehicles and to reduce the impact on the environment has generated new concepts, and the phrase "personal mobility" has become increasingly used in conjunction with the phrases "cooperative driving" and "environmental compatibility" [11], [12], [13]. Considered a necessity of social life, road traffic safety is influenced by the following factors: human factor (driver), technical factor (vehicle) and environmental factor (road, infrastructure, traffic and weather conditions) [14], [15], [16].

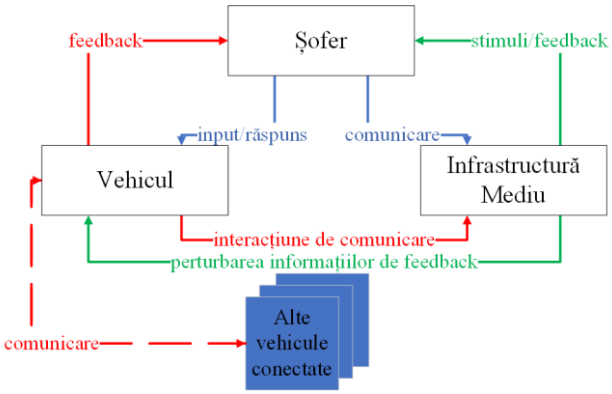

Figure 1. 2 Interaction of road traffic system components

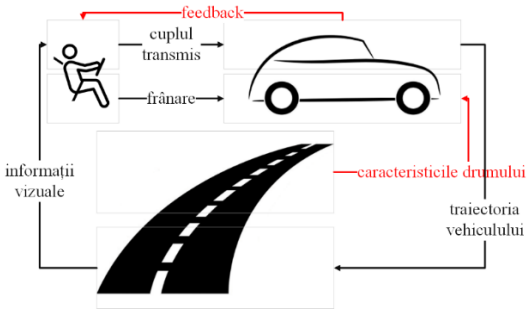

Figure 1. 3 Interconnection of road traffic system components

1.2.3 Characteristics of the components of the driver-vehicle-environment system

Variations in the states and characteristics of the components of the DVE system, determine the change in the parameters of these components and significantly influence the interaction between the driver-vehicle-environment (figure 1.8) [17], [18].

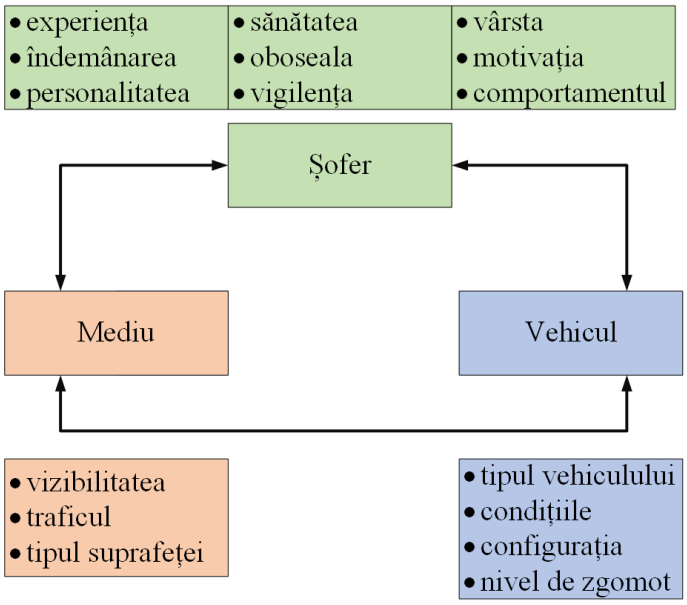

Figure 1. 4 Road traffic system parameters [19]

The purpose of advanced driver assistance systems is to reduce or even eliminate driver errors and increase the efficiency and safety of road traffic [20]. ADAS systems are developed to automate, adapt and improve vehicle systems for safer driving.

1.3 The current state of research on diagnosing the technical condition of vehicles

1.3.1 The importance and necessity of diagnosis

In the vehicles maintenance activity, the technical diagnosis involves both the determination of the technical condition and the evaluation of the results, consisting in the logical processing of the diagnosis conclusions (figure 1.9).

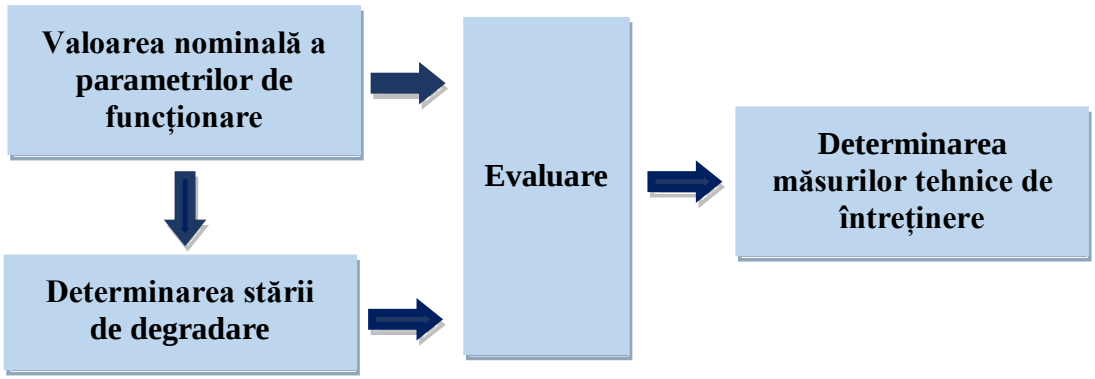

Figure 1. 5 The technical diagnostic process

1.3.2 The collection of the necessary information in the diagnostic process. Vehicle sensors

On board of modern vehicles it is necessary to measure physical quantities, an operation that is performed through a wide range of sensors [21]. Today's vehicle electronic systems are becoming increasingly complex, with electronic devices and software content integrated into applications ranging from simple door and window control to remote data transfer, between vehicles or between a vehicle and infrastructure.

1.3.3 Vehicles ”on board” diagnosis

Fault detection immediately after its occurence is performed by constantly monitoring the operation of vehicle systems, through on-board diagnostic (OBD) techniques and equipment. The information from the sensors reaches the electronic control units of the vehicles which establish the operating and adjustment parameters of the vehicle.

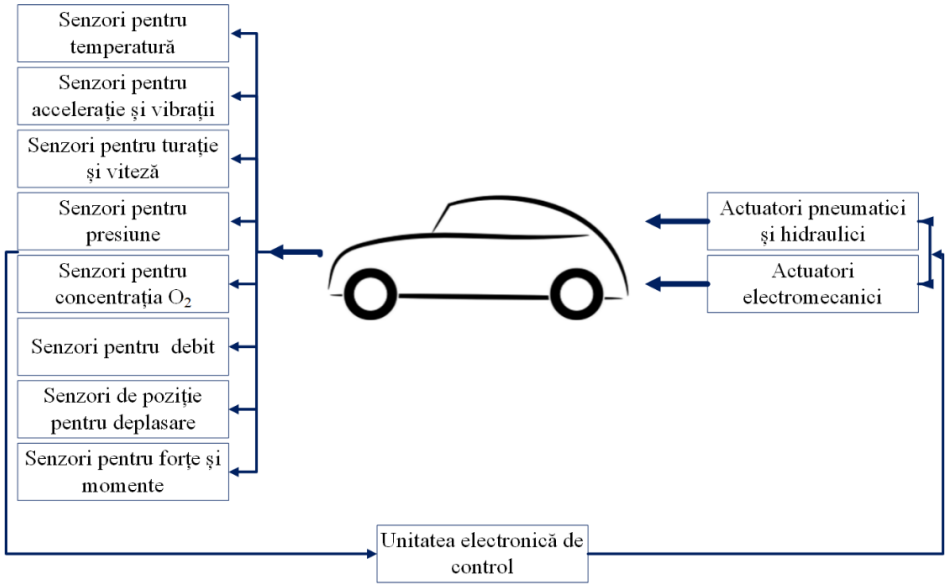

Figure 1. 6 Electronic control of vehicle systems

1.3.4 Expert systems for vehicle diagnostics

Dependence on a specialist can be minimized if his expertise is replaced by documentation in a computer system. Simultaneously with the rapid development of mobile devices such as PDAs (personal digital assistants), smartphones etc., an expert system combined with these mobile devices ensures the detection of faults and the diagnosis of the vehicle. ES provides powerful and flexible means to find solutions to a variety of problems that often cannot be solved by other traditional methods [22], [23].

1.4 Partial conclusions

The paper aims to develop a mobile diagnostic system to monitor the state parameters of vehicle systems during operation. The low level of training and knowledge in the automotive domain of some drivers, who do not notice certain symptoms of failures or the imminence of their occurrence, is an argument in favor of developing a mobile diagnostic system. The research aims to identify a method for diagnosing these defects in driving, having as a starting point the symptoms that an experienced driver perceives in driving (sounds, vibrations, abnormal shocks) [2], [3], [5], [6].

CHAPTER 2
THE INTERACTION BETWEEN THE VEHICLE AND THE ROADWAY. VEHICLE STEERING SYSTEM

2.1 The process of driving vehicles

The process of vehicle driving requires obtaining a controlled movement, in conditions of stability, allowed by its design, its main parameters and type of steering and suspension systems, grip, profile, inclination and condition of roadway, as well as other traffic specific factors [24], [25]. The driver skills and experience, combined with the actions of the Advanced Driver Assistance Systems (ADAS), implemented on the vehicle, are defining in making the necessary corrections, when the movement of the vehicle differs from the desired one or the one necessary to ensure road traffic safety.

2.2 Vehicle steering system. Role, construction and operation

The systemic approach to the formation of the vehicle gives a primary role to the steering system, along with the other component systems (suspension system, propulsion system, braking system, running system, etc.), in the process of vehicles optimum operation.

Representing an interface between the driver and the vehicle, the steering system fulfills two important functions: it ensures the registration of the vehicle on the ordered trajectory and transmits to the driver, during driving, by steering wheel movements or variations of the resistant moment to its actuation, information about the vehicle interaction with the roadway [26], [27], [28].

2.3 Steering wheel angles of the vehicle. Steering system geometry

Steering wheel angles have an important role in vehicle dynamics. They contribute to the stabilization of the vehicle on the trajectory, both in corners and straight, to reduce steering resistance, to maintain the direction of the vehicle in a straight line, to return the steering wheel to the upright position after the steering maneuver, to reduce the effect of forces disruptors acting on the steering wheels, the uniform wear of the tires, the compensation, within certain limits, of the clearances and the elasticity of the bushings in the suspension and steering systems [29], [30]. The specific angles of the steering wheels (figure 2.15) are divided into categories, as it follows:

a) wheel angles:
- wheels camber angle;
- wheel convergence angle;

b) pivot axis angles:
- angle of transverse inclination of the pivot axis (king pin or steering axis inclination);
- longitudinal inclination angle of the pivot axis (caster angle).

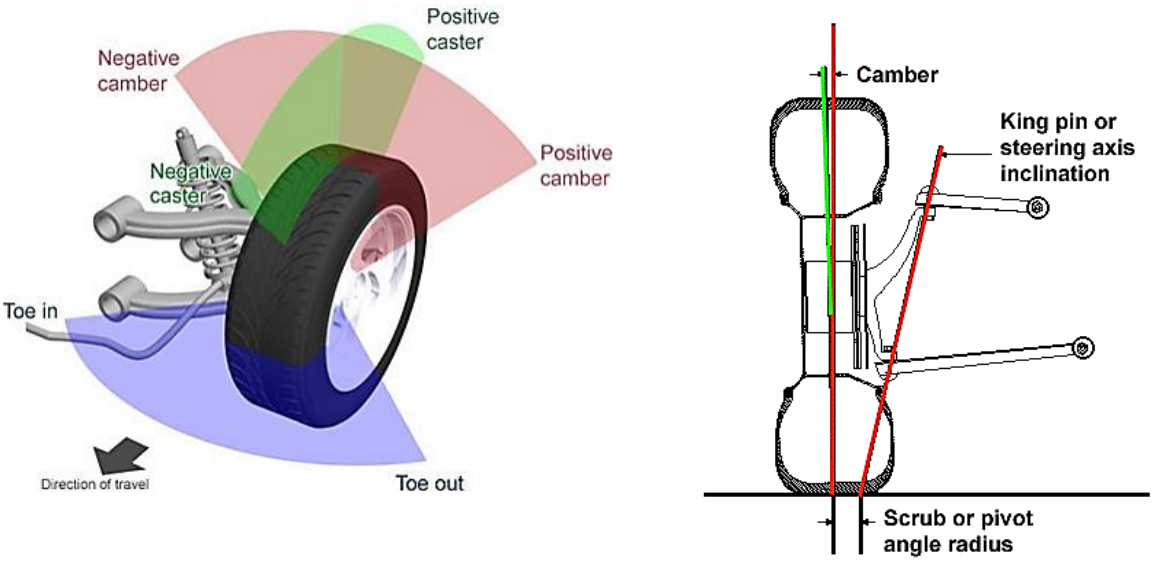

Figure 2. 1 Steering wheel specific angles [31], [32]

2.4 Vehicle suspension system

To achieve the objectives of maneuverability and stability of the vehicle, the steering system works with certain components of the suspension system to ensure the steering movement of the wheels. The MacPherson suspension system is the most common construction solution for mass-produced vehicles, due to its simple design, low number of parts and component subassemblies, as well as high reliability.

2.5 Diagnosis of the vehicles steering system

2.5.1 The requirement of the vehicles technical condition inspection. Legislation

The legislation in Romania stipulates that the certification of vehicle conformity, regarding road safety, environmental protection and classification in the category of use according to destination, is carried out, mandatory, by performing periodic technical inspection (I.T.P.). This operation is carried out, in accordance with the Regulations on the periodic technical inspection of vehicles registered or registered in Romania - RNTR 1, within the periodic technical inspection stations, whose authorization and monitoring is performed by the Romanian Auto Registry [33], [34].

2.5.2 Periodical technical inspection. Classification, empowered units, specific endowments

The current legal norms establish the organization and the operation of the vehicle periodic technical inspection system in Romania. The aim of the doctoral thesis is to develop a method for diagnosing spherical joint wear of the steering system, taking as a starting point the symptoms that an experienced driver perceives in vehicle driving (sounds, vibrations, abnormal shocks).

2.5.3 Steering system inspection

As a result of the steering system verification operations, excessive wear of the spherical joints may be detected, depending on the constructional characteristics of the vehicle, positioned as in figure 2.34.

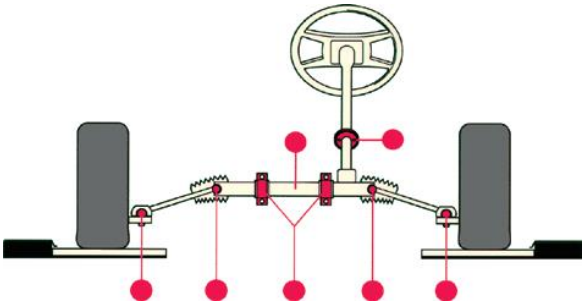

Figure 2. 2 Position of the spherical joints at which excessive wear can occur [35]

2.6 Partial conclusions

In the interval between two periodic technical inspections or two periodic inspections, defects may occur and an important role in their detection is played by the driver, with relative experience in diagnosing steering system failures. The road infrastructure, the degree of wear, the vehicles life service, as well as the driver experience, contribute substantially to the failure.

The driver lack of experience in detecting these faults can delay the diagnosis and replacement of a defective components, which can lead to accelerated wear and other parts and subassemblies within the steering system. This delay in carrying out diagnostics and specific maintenance operations leads to the operation of high-cost vehicles, but the high risk is to endanger traffic safety.

CHAPTER 3
METHODS AND INSTRUMENTS FOR STEERING SYSTEM DIAGNOSIS, USING VIBRATION ANALYSIS

3.1 Vehicles noise, vibrations and harshness

The process of operating vehicles involves their permanent exposure to sounds and vibrations, which are generated by both external and internal causes, which act simultaneously in running (figure 3.2).

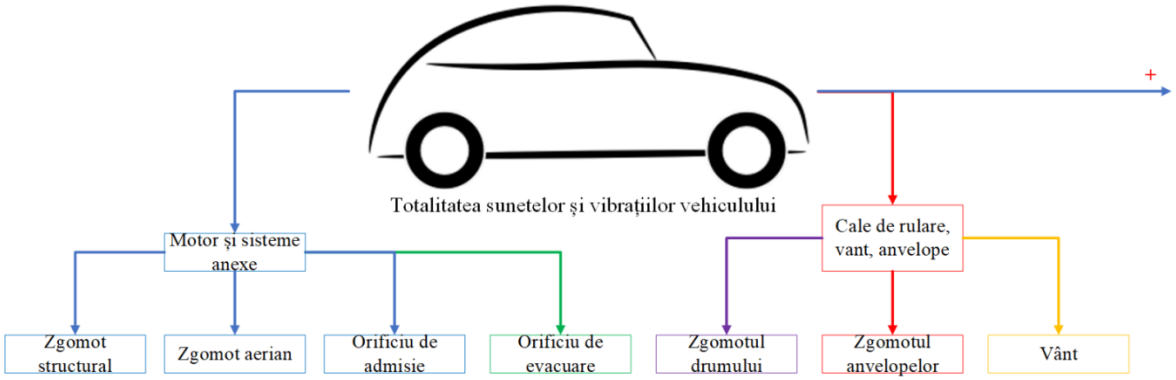

Figure 3. 1 Sounds and vibrations generating sources in vehicles [36]

3.2 Human sensory perception of vehicle-roadway interaction

The effects of shocks and vibrations, generated by the vehicles operation, are manifested both in the vehicle, by generating wear on the assemblies or component subassemblies, affecting their durability, and on the driver, affecting his physiological condition (fatigue, health, attention), the cumulative effect manifesting itself in terms of road safety, in the sense of reducing it [37], [38].

3.3 Vibration generating factors of vehicles. Vibration theory considerations

Random vehicle mechanical vibrations occur, when crossing road irregularities, when traveling on rough terrain, with pits, hard to reach or unpaved roads. The same vibrations or shocks can be perceived by the driver due to their transmission through the body and passenger compartment elements (floor, seat, dashboard etc.) [39], [40], [41] .

3.4 Methods, instruments and software for diagnosing spherical joints of the vehicle steering system

To perform the tests, a vehicle from category M1 was selected, frequently encountered in Romania, a Dacia Logan model, with the following technical characteristics: gasoline engine, cylinder capacity 1189 cm3, engine power 55 Kw, tire dimensions 185/65 R15, year of manufacture 2016, with a turnover of approximately 70,000 km, without defects. The measurements were performed using a DA20-RION 4-channel digital recorder with DA-20 VIEWER and CAT 78 WR data processing software - Version 4.018, as well as a Brüel & Kjær triaxial accelerometer, type 4321.

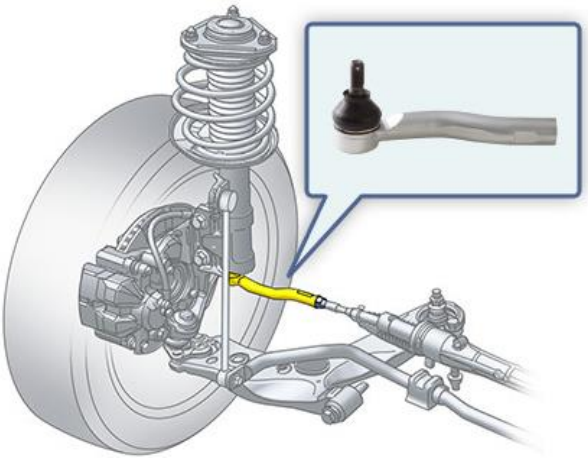

Figure 3. 2 Tie rod end [43]

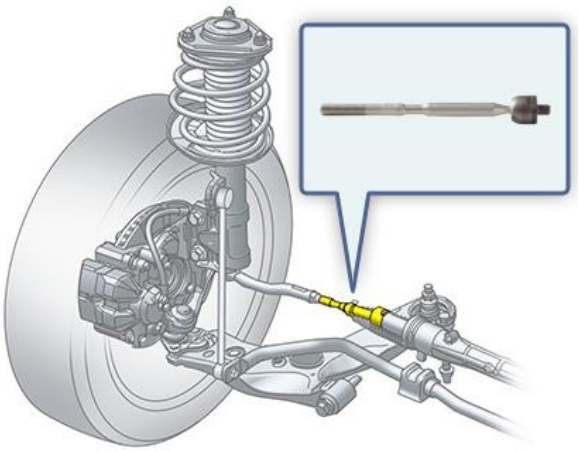

Figure 3. 3 Tie rod [43]

3.5 Partial conclusions

The researched diagnostic method is based on the fact that the driving over various bumps, frequent in urban traffic, determines the appearance of shocks in the defective spherical joints. The shocks produced in the defective tie rod excite natural modes of vibration of the tie rod-tie rod end assembly, the determination of the system response to these shocks being defining for the analyzed diagnostic method.

In order to establish the mark of the shocks produced in the defective spherical joints of the steering system, more precisely to the tie rod end, the research methods and tools aim to estimate the response to multiple shocks by using the finite element analysis program Ansys Workbench with Modal module. Vibration measurements of the tie rod end assembly on the test bench and performing tests on a vehicle in different driving conditions, with alternative mounting of a tie rod end with or without defect of the spherical joint and comparative analysis of the responses of the analyzed system, with and without defect, at different sources of excitations.

CHAPTER 4
THE ESTIMATION OF SHOCK RESPONSE BY FINITE ELEMENT MODELING

4.1 Geometry of the tie rod – tie rod end assembly

Natural vibration analysis involves determining the natural frequencies and the modes of the tie rod - tie rod end assembly in the steering system of the Dacia Logan, an analysis that was performed using the Ansys Workbench finite element analysis program. The 3D geometry of the analyzed assembly was performed using the Catia V5 program and exported as a step extension file in Ansys Workbench.

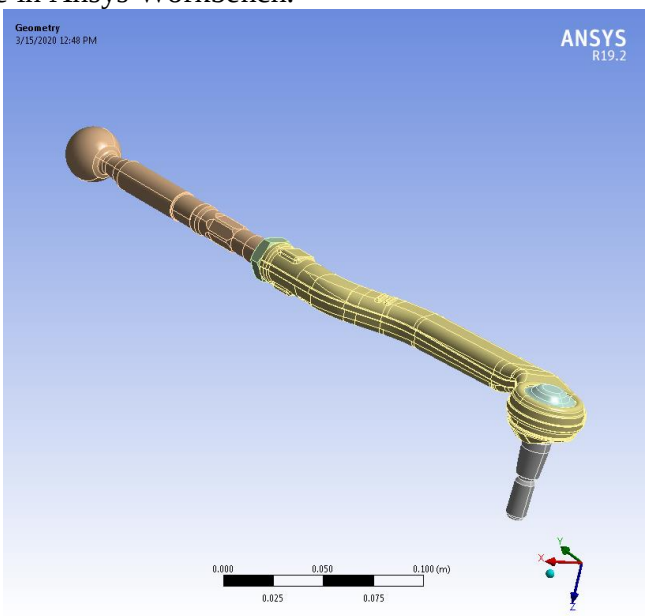

Figure 4. 1 3D Geometry of the steering tie rod - tie rod end assembly

4.2 Characteristics of component materials. Discretization with finite elements. Connection conditions

The characteristics of the materials from which the components of the modeling subassembly are made were established by analyzing the sectional structure of the tie rod end (figure 4.5) and by consulting specific standards and catalogs.

Figure 4. 2 Dacia Logan tie rod end section

The discretization of the steering tie rod – tie rod end model was performed with solid elements, with the type of SOLID 187 element from the Ansys program library, this being an element with 10 nodes and 3 degrees of freedom per node, representing the translations on the 3 coordinate axes. Thus, for the 3D geometry of the analyzed system 66734 nodes and 37784 elements were defined (figure 4.3)

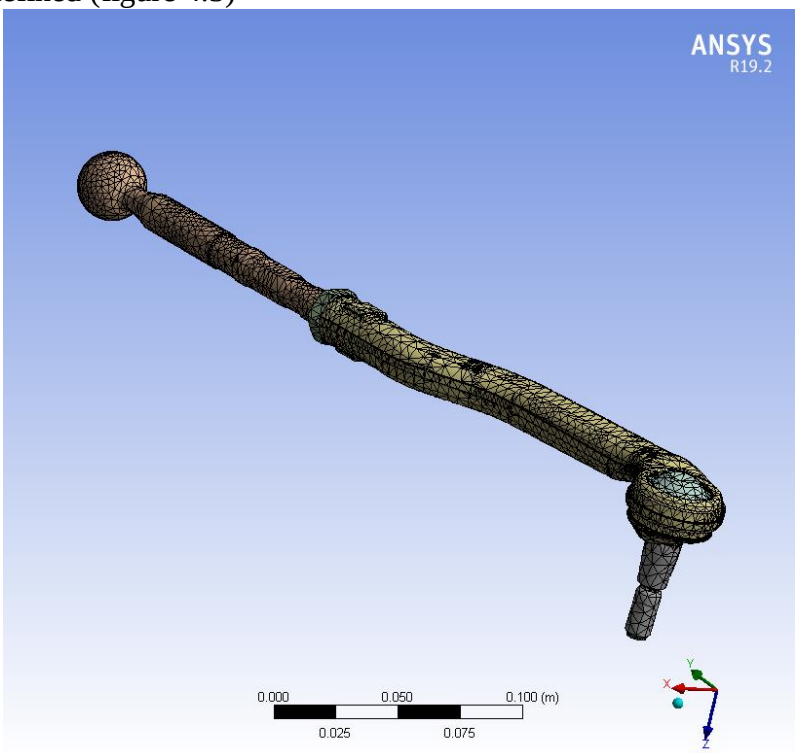

Figure 4. 3 Discretization of the system with solid elements

4.3 Analysis of the wear in the spherical joint. Wear measurement. Maximum wear and stress directions

To make the measurements of the clearance in the spherical joint of the tie rod end, the device in figure 4.8 was made, and the measurements were performed by fixing the tie rod - tie rod end assembly in the device and measuring the clearance in the longitudinal direction of the assembly (transverse to the vehicle), steering on which the wear of the spherical joint is maximum.

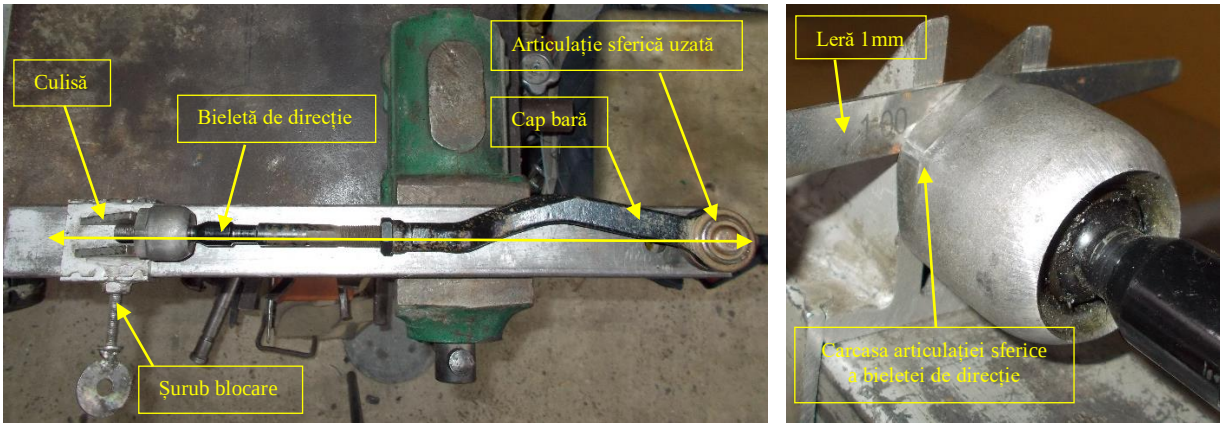

Figure 4. 4 Device for clearance measuring in the spherical joint of the tie rod end

Figure 4. 5 Cross-sectioned tie rod end

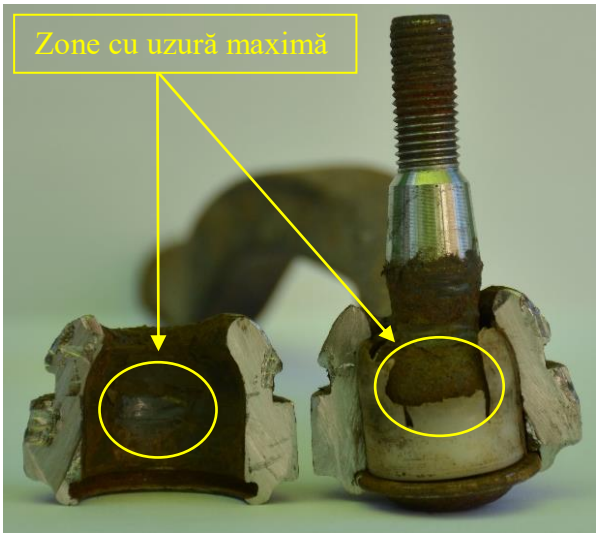

Figure 4. 6 Cross-sectioned tie rod end

4.4 Natural vibration analysis of the system

The study of natural vibrations in the Ansys Workbench program focused on the situations encountered during running, namely that of non-existence of the defect (without default in the spherical joint) or that with clearance having values in the measuring range (0-1 mm / radius), found as a result of measurements performed on the batch of 10 used tie rod end. As a result, simulations of dynamic response were performed for system with or without defect in the spherical joint with the following values: 1 micron / radius, 0.1 mm / radius, 0.5 mm / radius, 1 mm / radius.

The first simulations were performed for the situation of flawless tie rod - tie rod end assembly.

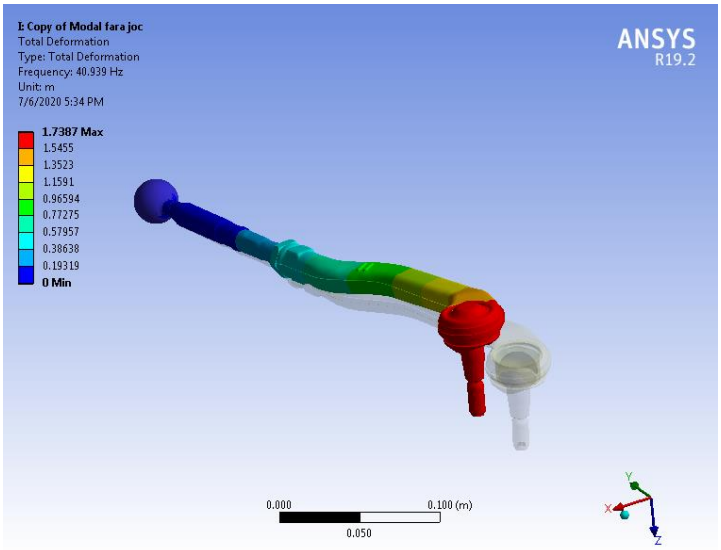

Figure 4. 7 System without defect (vibration mode 1 - frequency 40.939 Hz)

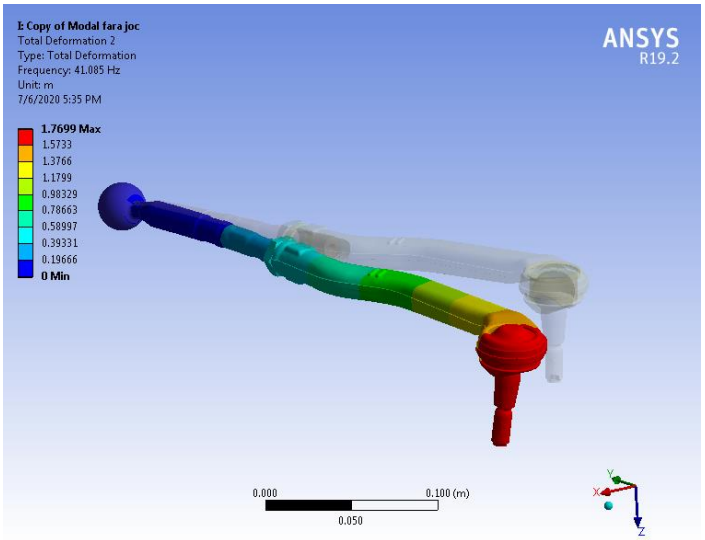

Figure 4. 8 System without defect (vibration mode 2 - frequency 41.085 Hz)

The following simulations were performed for the situation in which the tie rod - tie rod end assembly has a clearance in the spherical joint, with a value of 1 mm / radius.

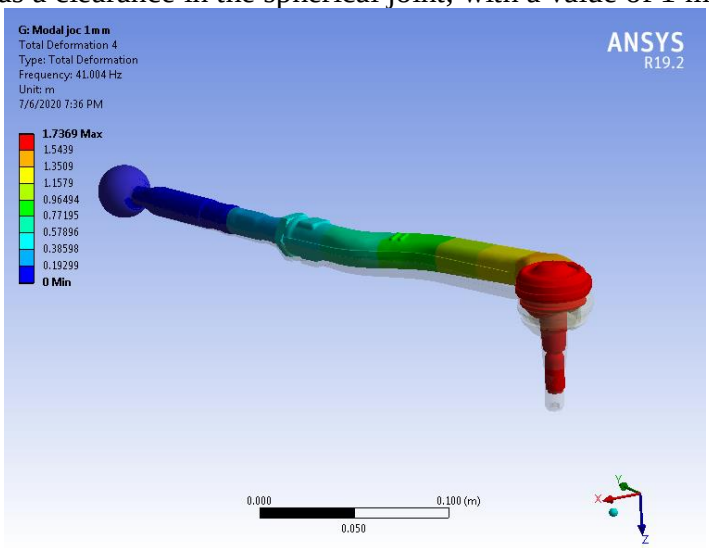

Figure 4. 9 System with clearance of 1mm / radius (4 vibration mode - frequency 41.004 Hz)

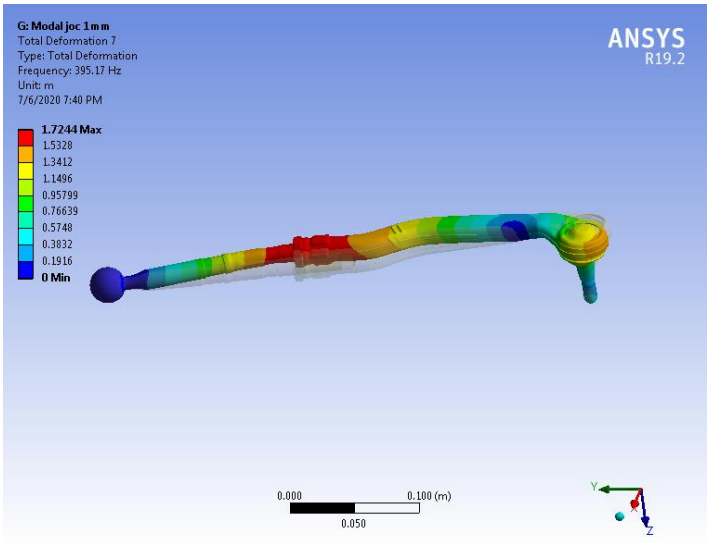

Figure 4. 10 System with clearance of 1mm / radius (vibration mode 7 - frequency 395.17 Hz)

Table 4. 1 The natural frequencies of the studied system according to the size of the clearance between the spherical pivot and the teflon bush

No. natural vibration mode	**Frequencies of the system (Hz)**				
	Flawless	**Clearance value**			
		1micron/rază	0,1mm/rază	0,5mm/rază	1mm/rază
	1	**2**	**3**	**4**	**5**
1	40,939	6,3896	6,1824	5,0469	3,6043
2	41,085	10,271	9,8523	8,3503	6,1684
3	126,08	29,924	26,989	21,043	16,127
4	215,63	41,005	41,005	41,004	41,004
5	349,74	42,756	42,754	42,744	42,731
6	395,6	351,83	351,81	351,78	351,59
7	598,57	395,26	395,26	395,23	395,17
8	1028,7	596,11	596,06	595,98	595,49
9		1036,3	1036,2	1034,5	1025,1

4.5 Partial conclusions

The analysis of the data in table 4.2 reveals that the appearance of the clearance and the increase of its value in the spherical joint leads to the decrease of the values of the natural frequencies, specifically in case of the first natural frequency [44].

The dynamic analysis of the natural modes and of the corresponding frequencies of the tie rod - tie rod end assembly, highlights the fact that the quantities that *"control"* the first natural frequency of the system are:

- the elasticity modulus of the bushing material (the higher the elasticity modulus, the higher the fundamental natural frequency);
- the clearance value in the spherical joint (the higher the clearance, the lower the fundamental natural frequency).

CHAPTER 5
RESPONSE DETERMINATION TO THE SHOCK APPLIED TO THE SYSTEM ON THE TEST BENCH

5.1 Methods and means of testing

The vibration tests of the tie rod - tie rod end assembly performed on the test bench aimed to determine the response of the defective system (defect in the spherical joint) to single or multiple shocks applied in the spherical joint of the tie rod end. The casing of the tie rod end was fixed in the vise, thus simulating the connection with the rack of the steering gear (figure 5.1). Thus, the same conditions of connection as those established for finite element modeling were met.

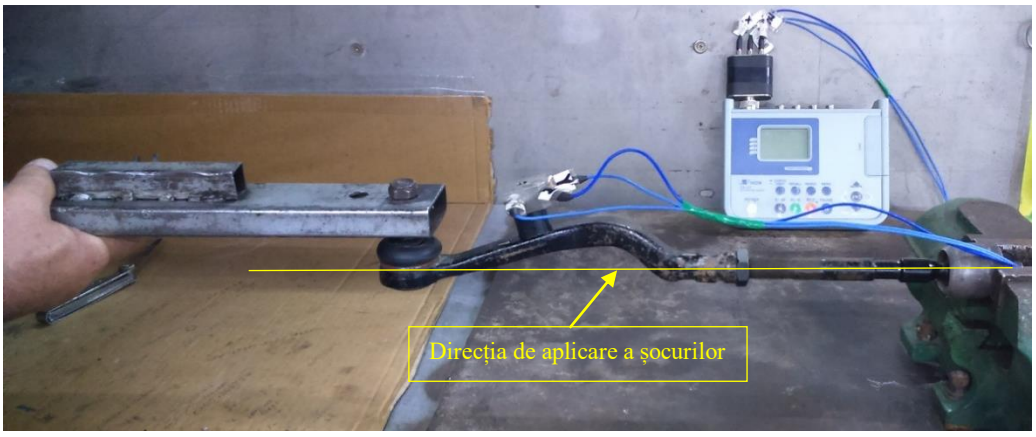

Figure 5. 1 The devices position on the test bench

Table 5. 1 Bench test conditions

Test no.	The technical state of spherical joint	Frequencies domain	Range	Aplied shocks details	Obs.
B1	defective spherical joint	0-100 Hz	axis x,y,z 3,2E+1	one/simple shock	compare simple shock / multiple shocks
B2	defective spherical joint	0-100 Hz	axis x,y,z 3,2E+1	multiple 1beat/2-3 sec	
B3	defective spherical joint	0-500 Hz	axis x,y,z 3,2E+2	one/simple shock	compare simple shock / multiple shocks
B4	defective spherical joint	0-500 Hz	axis x,y,z 3,2E+2	multiple 1beat/2-3 sec	
B5	defective spherical joint	0-1000 Hz	axis x,y,z 3,2E+2	one/simple shock	compare simple shock / multiple shocks
B6	defective spherical joint	0-1000 Hz	axis x,y,z 3,2E+2	multiple 1beat/2-3 sec	

5.2 Experimental results of bench tests

The vibrational analysis was performed by comparing the defective system responses to simple shock and to multiple shocks, in the ranges of 0-100 Hz, 0-500 Hz and 0-1000 Hz.

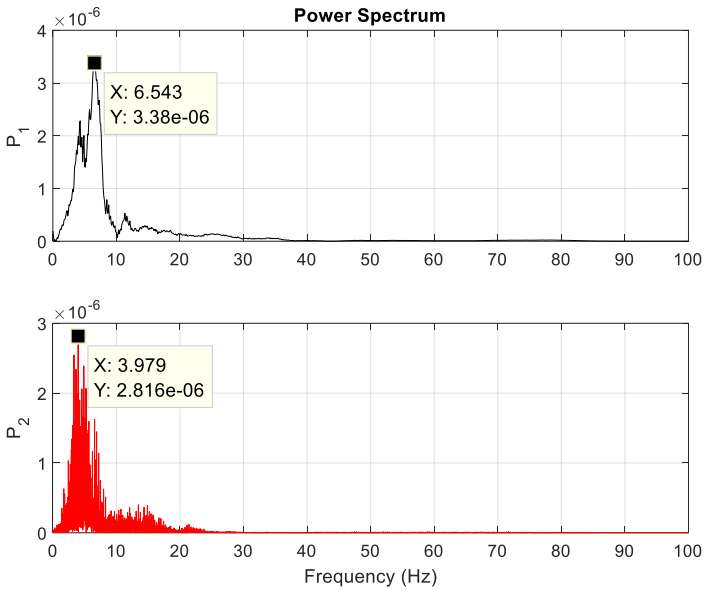

Figure 5. 2 Periodograms OX axis in the range of 0-100 Hz: (a) single shock; (b) multiple shocks

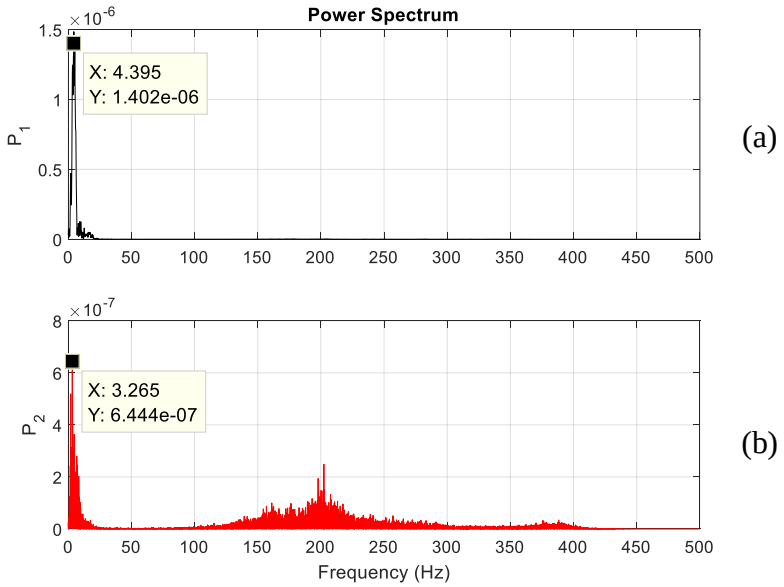

Figure 5. 3 Periodograms OX axis in the range 0-500 Hz: (a) single shock; (b) multiple shocks

In order to be able to compare the responses to single shock and multiple shocks, the audio signals with the same sampling frequency were concatenated in this order and the STFT function was applied to the sum signal. Thus, the simple and multiple shock response spectrograms resulted, corresponding to the processing of the recordings made in the 0-500 Hz frequency range, related to the B3 and B4 tests, on the OX, OY and OZ axes.

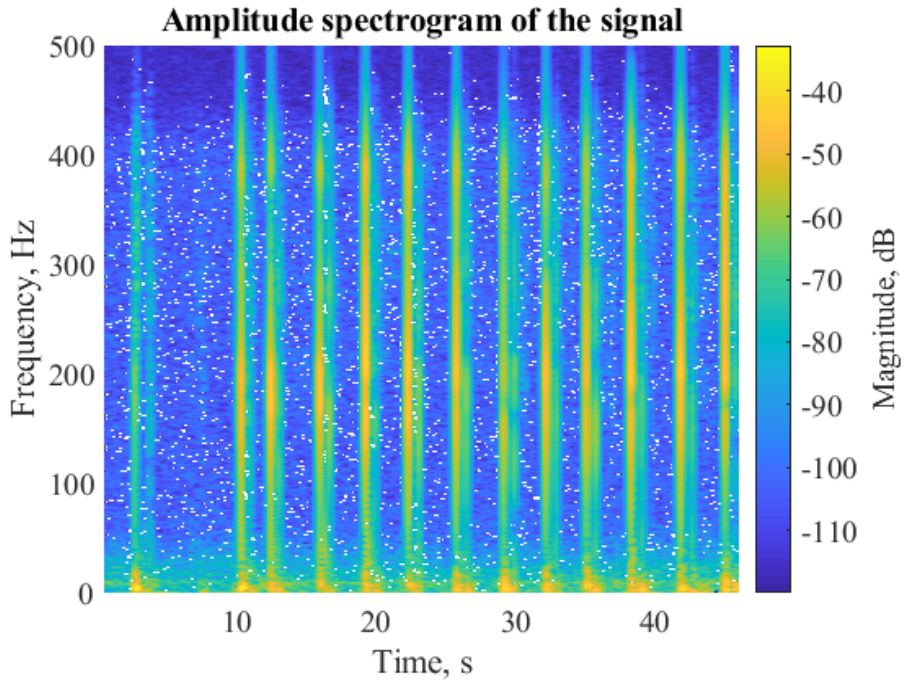

Figure 5. 4 STFT spectrogram for single (B3 test) and multiple (B4 test) shock response OX axis

5.3 Partial conclusions

Both data processing procedures in Matlab (periodogram generation function and STFT function) lead to results similar to those obtained after finite element simulation in terms of frequency (with the value of 5 Hz) which characterizes its natural fundamental vibration mode of the analyzed system, namely the one with clearance in the spherical joint of 0.5 mm / radius. Also, similar results were obtained from the finite element analysis on the other natural vibrations modes of the system with frequency values up to 1000 Hz, approximately of 350 Hz, 400 Hz and 600 Hz. The response of the system to the shock must be analyzed by identifying vibrations specific to the existence of the defect in frequencies domain and not by attempting to identify single vibration frequency, with well-defined values, as in the case of stationary vibrations. Thus, by using STFT we obtain a mark of the dynamic behavior of the shock system, in the form of vertical bands, with high energy loads in certain frequency ranges, specific to the spectrograms of percussion music systems [45], [46], [47].

CHAPTER 6
RESPONSE DETERMINATION TO THE SHOCK APPLIED TO THE SYSTEM DURING VEHICLE RUNNING

6.1 Description of the experiment

The tests were performed in different driving conditions, with the alternative mounting of a tie rod end, with or without defect of the spherical joint. The objectives of the tests were to establish the dynamic vibration mark and perform a comparative analysis of the responses of the analyzed system, with and without defects, when driving on different routes, over different types of bumps and at different engine and vehicle speeds.

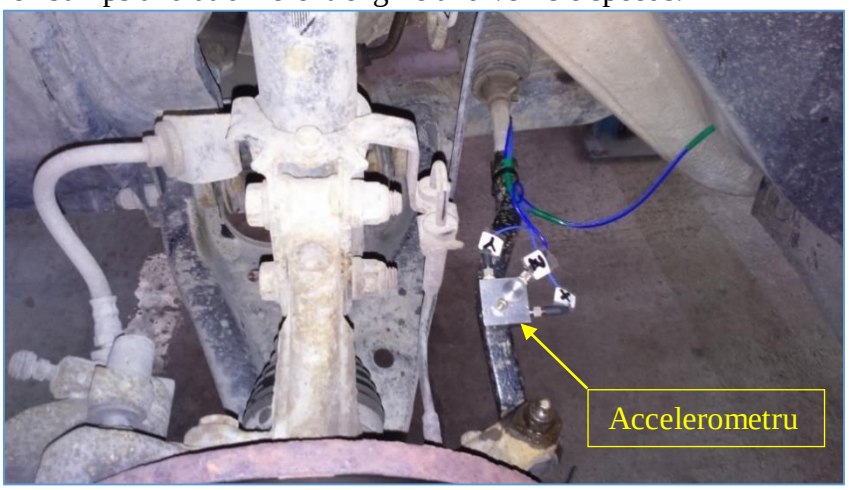

Figure 6. 1 Positioning the accelerometer on the left tie rod end

Shocks produced during driving both between the vehicle and the road, internal shocks also, produced between components (subassemblies) of the vehicle, generate random vibrations, non-stationary, characterized by laws of motion expressed by statistical and probabilistic parameters. This category includes the vibrations generated by the shocks in the spherical joint of the defective tie rod end, shocks whose probability of production increases when driving through various bumps of the driveway.

Table 6. 1 Running test conditions

Nr. test	Starea articulației sferice	Tip rulaj/cale de rulare	viteză de deplasare (km/h) / treapta de viteză	Turație motor rot/min	Sens de deplasare	Range	Obs.
test 1	cu defect	rectiliniu/ rulaj peste capace de canalizari	30 km/h, treapta a III-a	1500	Bucurestii Noi- str. Tecuci	axele x,y,z 3,2E+2	teste de comparat, cu și fără defect
test 2	fără defect		30 km/h, treapta a III-a	1500	Bucurestii Noi- str. Tecuci	axele x,y,z 1,0E+2	
test 3	cu defect	rectiliniu/ rulaj peste capace de canalizari	30 km/h, treapta a III-a	1500	Posta Veche- Bucovinei	axele x,y,z 3,2E+2	teste de comparat, cu și fără defect
test 4	fără defect		30 km/h, treapta a III-a	1500	Posta Veche- Bucovinei	axele x,y,z 1,0E+2	
test 5	cu defect	rectiliniu/ rulaj peste capace de canalizari	30 km/h, treapta a III-a	1500	Lozoveni- Peco Rojevas	axele x,y,z 3,2E+2	teste de comparat, cu și fără defect
test 6	fără defect		30 km/h, treapta a III-a	1500	Lozoveni- Peco Rojevas	axele x,y,z 1,0E+2	
test 7	cu defect	rectiliniu/ rulaj peste capace de canalizari	25 km/h, treapta a III-a	1250	Peco Rojevas - Lozoveni	axele x,y,z 3,2E+2	teste de comparat, cu și fără defect
test 8	fără defect		25 km/h, treapta a III-a	1250	Peco Rojevas - Lozoveni	axele x,y,z 1,0E+2	
test 9	cu defect	rectiliniu/ rulaj peste capace de canalizari	40 km/h, treapta a IV-a	1500	str. Tecuci - Bucurestii Noi	axele x,y,z 3,2E+2	teste de comparat, cu și fără defect
test 10	fără defect		40 km/h, treapta a IV-a	1500	str. Tecuci - Bucurestii Noi	axele x,y,z 1,0E+2	
test 11	cu defect	rectiliniu/ rulaj peste linii tramvai	20 km/h, treapta a II-a	1200	Prelungirea Brailei - Minion	axele x,y,z 3,2E+2	teste de comparat, cu și fără defect
test 12	fără defect		20 km/h, treapta a II-a	1200	Prelungirea Brailei - Minion	axele x,y,z 1,0E+2	
test 13	cu defect	rectiliniu/ denivelari usoare	40 km/h, treapta a IV-a	1500	Galati- Barbosi	axele x,y,z 3,2E+2	teste de comparat, cu și fără defect
test 14	fără defect		40 km/h, treapta a IV-a	1500	Galati- Barbosi	axele x,y,z 1,0E+2	
test 15	cu defect	rectiliniu/ denivelari usoare	40 km/h, treapta a IV-a	1500	Barbosi- Galati	axele x,y,z 3,2E+2	teste de comparat, cu și fără defect
test 16	fără defect		40 km/h, treapta a IV-a	1500	Barbosi- Galati	axele x,y,z 1,0E+2	
test 17	cu defect	rectiliniu/ denivelari usoare	30 km/h, treapta a III-a	1500	Galati- Barbosi	axele x,y,z 3,2E+2	teste de comparat, cu și fără defect
test 18	fără defect		30 km/h, treapta a III-a	1500	Galati- Barbosi	axele x,y,z 1,0E+2	
test 19	cu defect	rectiliniu/ denivelari usoare	30 km/h, treapta a III-a	1500	Barbosi- Galati	axele x,y,z 3,2E+2	teste de comparat, cu și fără defect
test 20	fără defect		30 km/h, treapta a III-a	1500	Barbosi- Galati	axele x,y,z 1,0E+2	

To determine the response of the system to shocks in the defective spherical joint of the tie rod end, the processing and analysis of recorded data in the frequency range of 0-500 Hz was performed comparatively, for each of the 10 pairs of tests, by the following methods: STFT analysis, Spectral Kurtosys analysis and spectral analysis in the time domain.

6.2 Data processing and analysis using the Short Time Fourier Transform procedure from the Matlab program

Since the shock response signals are non-stationary signals, the data recorded after performing the 20 tests in running were processed with the Short Time Fourier Transform analysis procedure, implemented within the Matlab program, thus resulting representations of frequency spectra of signals that vary over time.

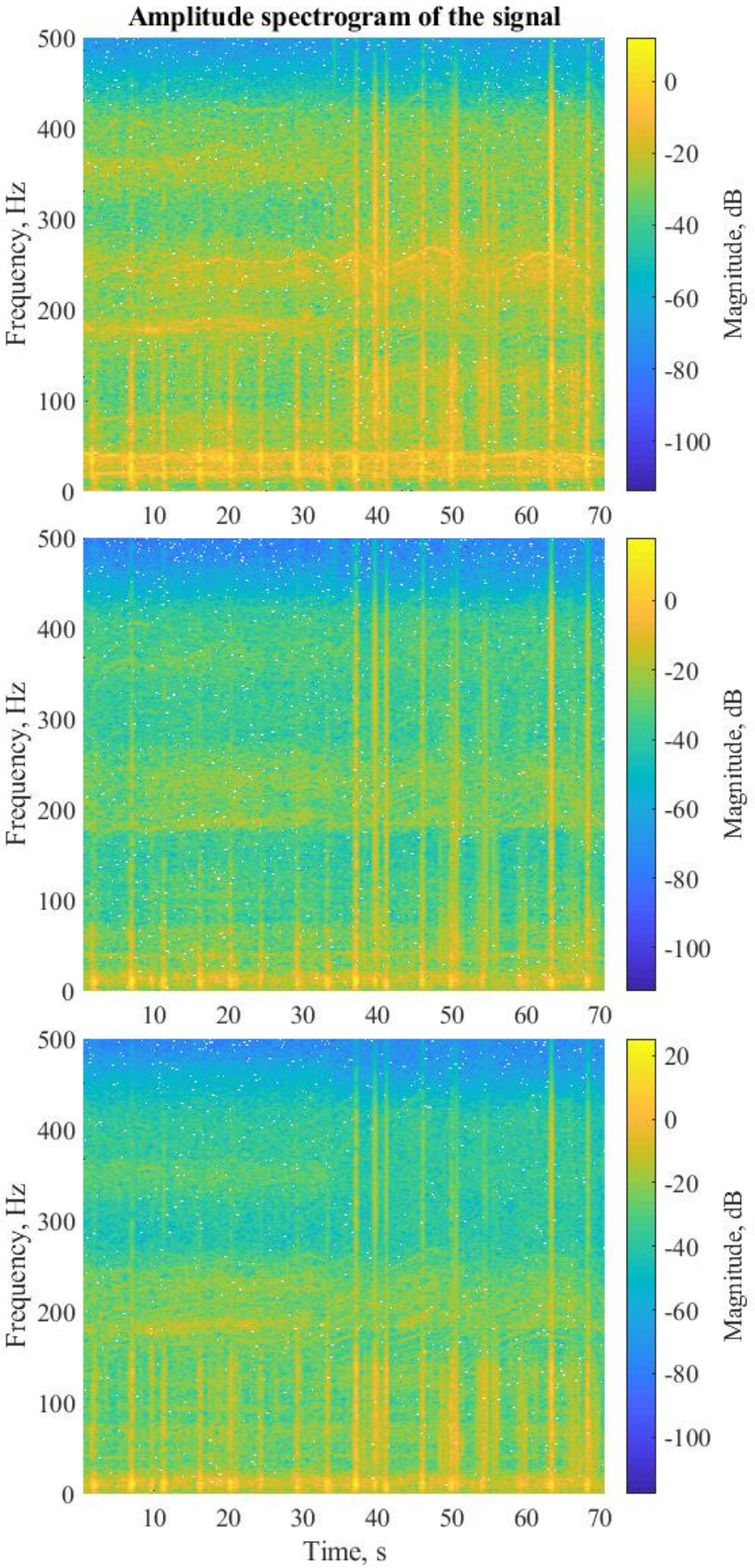

Figure 6. 2 Spectrograms of the response signal for test 4 (without defect) concatenated with test 3 (with defect): (a) on the OX axis; (b) on the OY axis; (c) on the OZ axis

Figure 6. 3 Street sewer covers in tests 3 and 4 - Poșta Veche Street [48]

In conclusion, the analysis of the spectrograms indicates that the running system response corresponds to both stationary vibrations (generated by engine operation and tire-driveway interaction), visible as continuous horizontal waves, and non-stationary vibrations in the form of vertical bands, corresponding to shocks, similar to those highlighted by bench tests. The mark of the shocks analyzed for diagnosis is that represented by the vertical bands with higher energy loads, in the range of 100-400 Hz.

6.3 Processing of recorded data in running and spectral analysis of signals using Kurtosis

Spectral kurtosis (SK) is a statistical quantity that can highlight non-stationary characteristics in the frequency range, considering its low values at frequencies for which stationary components (Gaussian) are present in the signal and high positive values at frequencies for which transients occur [49], [50]. This capability of spectral kurtosis (SK) is useful in detecting and extracting non-stationary signal components, corresponding to the operation of a faulty system [51], [52], [53], [54], [55], [56]. Spectral kurtosis, written as *K (f)*, of a signal *x (t)*, can be determined based on a STFT of a signal, *S (t, f)*:

$$S(t,f) = \int_{-\infty}^{+\infty} x(t) \cdot w(t-\tau) e^{-2\pi f t} dt \tag{6.6}$$

where *w (t)* is the window function of the STFT transformation

$$K(f) = \frac{\langle |S(t,f)|^4 \rangle}{\langle |S(t,f)|^2 \rangle^2} - 2 \tag{6.7}$$

where $f \neq 0$, and $\langle \cdot \rangle$ is the time mediation operator.

The scheme of applying the spectral kurtosis function K (f) on a signal x (t) is presented in figure 6.14.

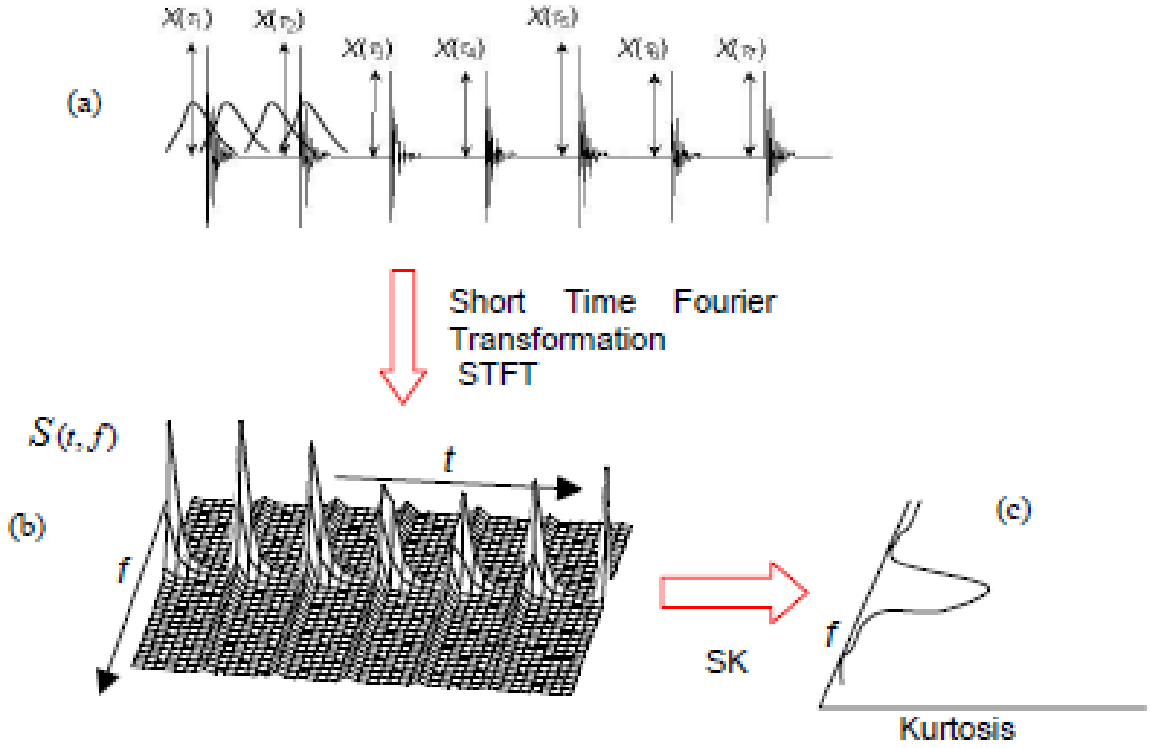

Figure 6. 4 a) Time signal; b) The result of the STFT transformation; c) Spectral kurtosis as a function of frequency [145]

The spectral kurtosis of a signal can be determined with the Matlab sequence:

$$sk = pkurtosis(x, fs, wo, 'ConfidenceLevel', p) \quad (6.8)$$

where: x = signal in the time domain, fs = sampling frequency, wo = optimal window length, p = confidence level for stationary signal components (values between 0 and 1).

A particular importance in highlighting the non-stationary components of the signal is the establishment of the optimal length of the "wo" window. For this purpose, in the Matlab program there is the possibility to determine the optimal length "wo" of the window, as well as the positioning in the frequency range of the transient components with high values of kurtosis, by means of a kurtogram (spectrogram). From these kurtograms are extracted the optimal window lengths (Optimal Window Length) corresponding to the frequency component of the signal with the highest kurtosis, lengths that will be used in the calculation of spectral kurtosis, to identify the transient components of the signal [57].

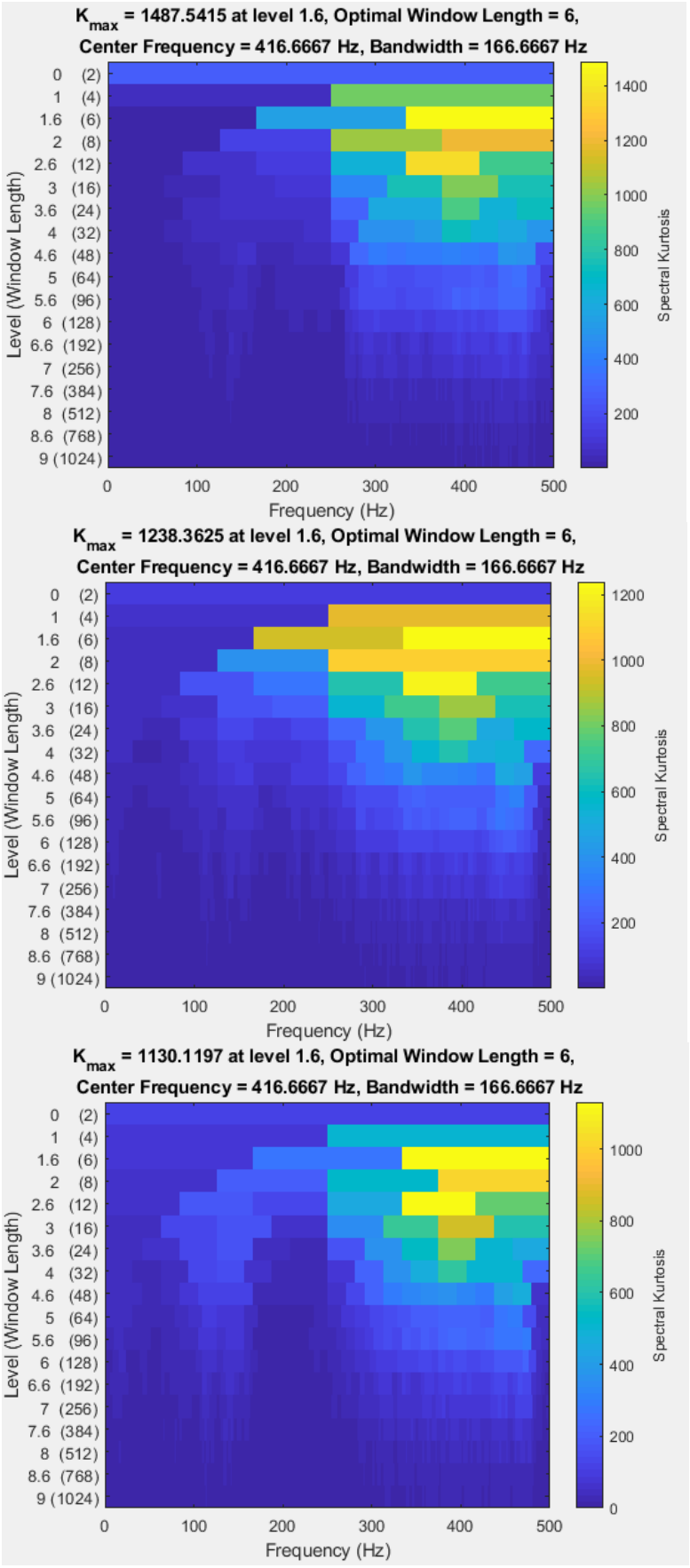

Figure 6. 5 Kurtograms of defective system response, test 3: (a) on the OX axis; (b) on the OY axis; (c) on the OZ axis

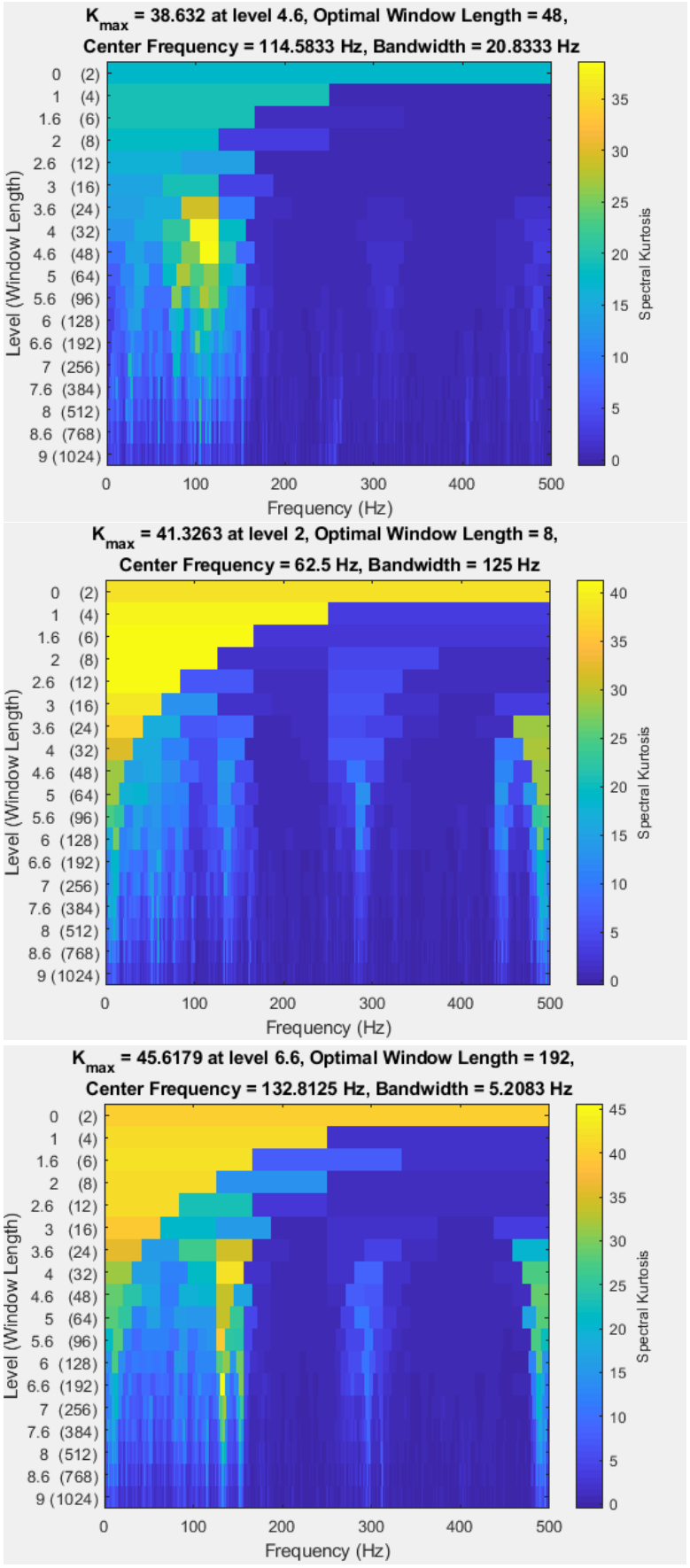

(a)

(b)

(c)

Figure 6. 6 Kurtograms of flawless system response, test 4: (a) on the OX axis; (b) on the OY axis; (c) on the OZ axis

The analysis of the kurtograms reveals the following conclusions:

- the optimal lengths of the windows extracted from the kurtograms corresponding to the defective signals have low values, comprised in the range of 6 - 8 and the high values of the afferent kurtosis confirm the high non-stationary level of the defective signal;

- kurtograms corresponding to flawless signals are characterized by high values of the optimal length of the windows, while kurtosis registers significant decreases, compared to the defective tests.

With the optimal window lengths determined by the kurtograms, the kurtosis of the spectral components is determined, taking into account a limit imposed in determining the stationary components by a confidence level. Spectral kurtosis variations were obtained for optimal WO lengths of the windows extracted from the kurtograms corresponding to each signal.

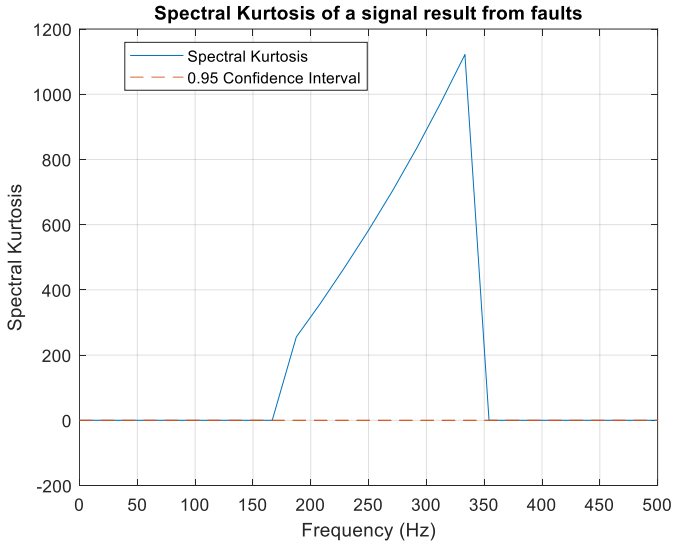

(a)

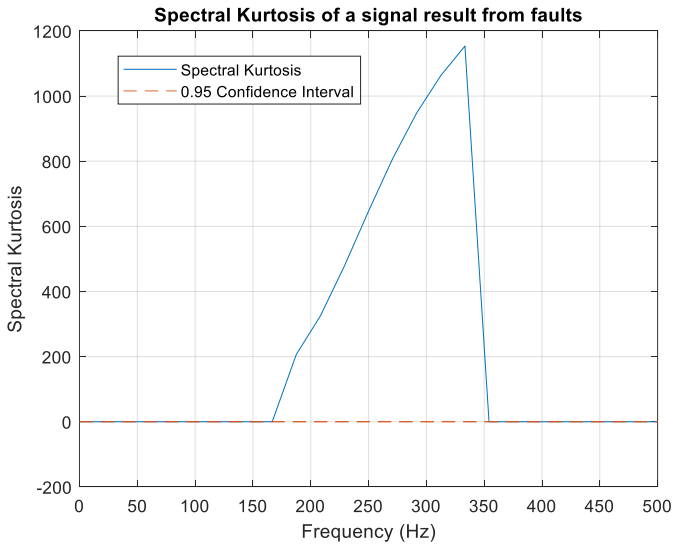

(b)

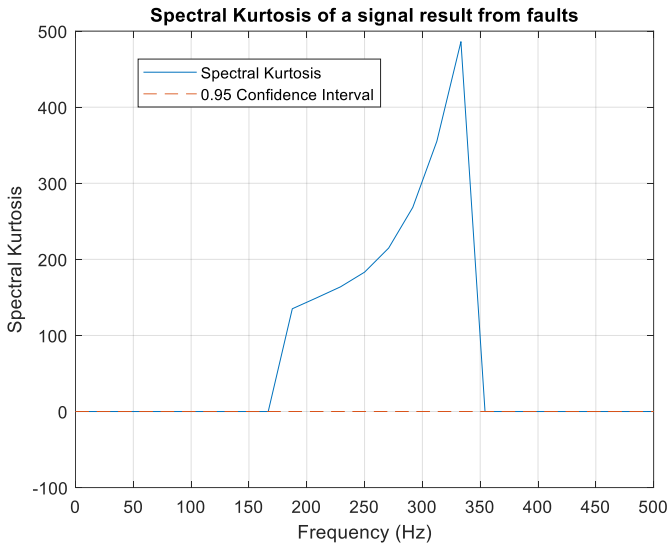

(c)

Figure 6. 7 Kurtosis variation for defective signal components, test 3: (a) on the OX axis, WO = 6; (b) on the OY axis, WO = 6; (c) on the OZ axis, WO = 6

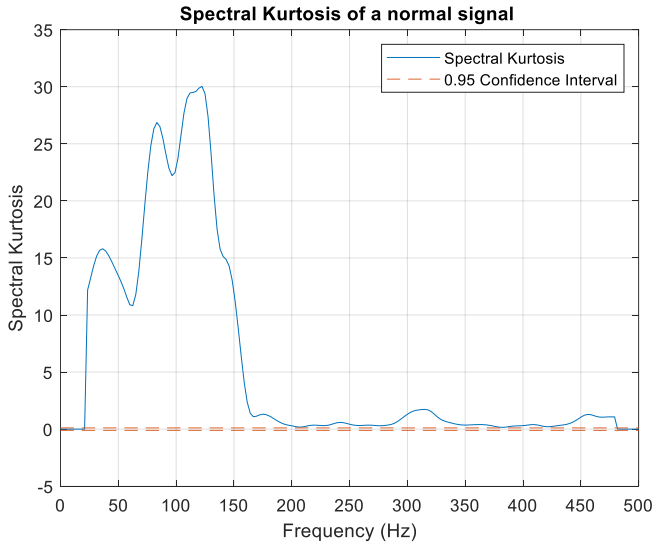

(a)

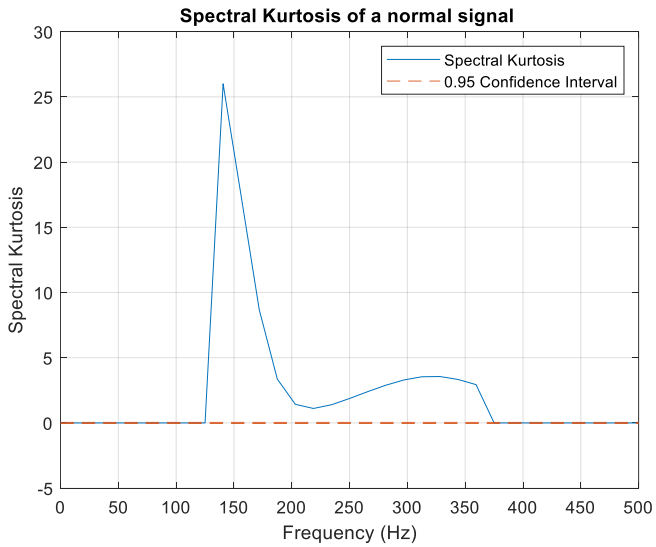

(b)

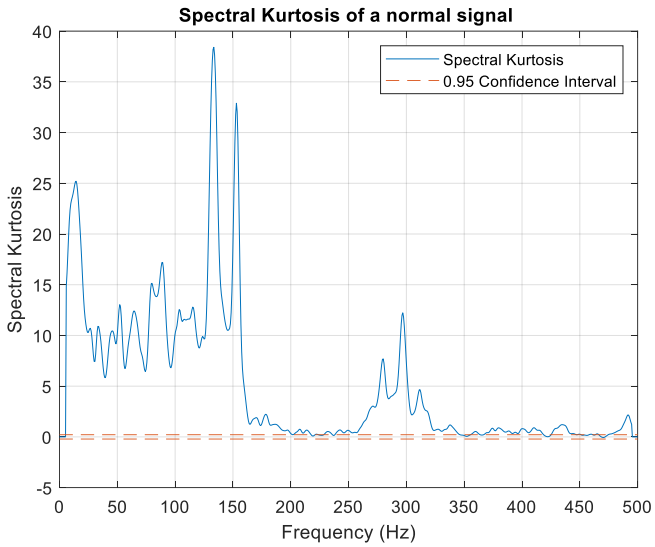

(c)

Figure 6. 8 Kurtosis variation for flawless signal components, test 4: (a) on the OX axis, WO = 48; (b) on the OY axis, WO = 8; (c) on the OZ axis, WO = 192

Spectral kurtosis analysis shows that both flawless and defective signals are non-stationary, but in the case of defective signal, the transient components of the signal have very high kurtosis values (maximum value of 1487.54) for a very small window length (in most records value of 6) with a magnitude corresponding to a shock. The presence in the recorded response of natural frequencies identifies the existence of a multiple shock, which excites several natural frequencies of the system.

The resulting data showed that the variation of kurtosis can be used to form a selection filter of that part of the signal recorded corresponding to the shock and, implicitly, the occurrence of the defect, considerably reducing the background noise and improving the diagnostic capacity. Since the wear of the tie rod end is characterized by short pulses represented by the multiple shocks between the component elements, the spectral kurtosis is useful for determining the frequency bands dominated by the error signals of the tie rod end, containing excited frequencies by failures.

6.4 Identification of the defective dynamic systems based on recorded data

6.4.1 Overview

In practice, we frequently encounter systems with a nonlinear behavior, corresponding situation to the analyzed steering system, with or without defect at the spherical joint of the tie rod end. Using polynomial models, models of dynamic systems from measured data can be identified. These polynomial models implemented in Matlab are ARX ("Auto Regressive with Exogenous input"), BJ ("Box-Jenkins") and OE ("Output Error"). With the recorded input-output data, several models were identified, and the one that allowed an adequate overlap of the measured data with the estimated data was the Box-Jenkins polynomial model [58], [59].

6.4.2 Development of the Box-Jenkins mathematical model of the dynamic system in the Matlab program

The syntax in Matlab for using the Box-Jenkins model is:
m = bj(data,orders)
m = bj(data,'nb',nb,'nc',nc,'nd',nd,'nf',nf,'nk',nk)
m = bj(data,orders,'Property1',Value1,'Property2',Value2,...)
the **bj** function returns the model **m** as a polynomial function (**idpoly**) with estimated parameters. The data reprezent an object that contains the input-output data.
The general shape of the Box-Jenkins model is:

$$y(t) = \sum_{i=1}^{nu} \frac{B_i(q)}{F_i(q)} u(t-nk) + \frac{C(q)}{D(q)} e(t) \tag{6.9}$$

where *nu* is no number of input channels.

For an input - u (t) and an output - y (t), the general shape of the Box-Jenkins model is:

$$y(t) = \frac{B_i(q)}{F_i(q)} u(t-nk) + \frac{C(q)}{D(q)} e(t) \tag{6.10}$$

The Box-Jenkins model can be represented as a data stream as in figure 6.27, where u(k) - the input signal, y(k) - the output signal and e(k) - the integrated noise signal.

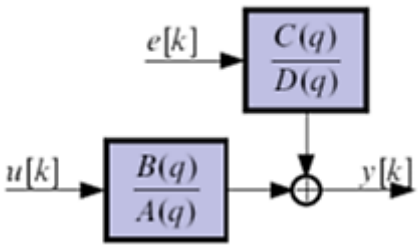

Figure 6. 9 Data flow in the Box-Jenkins model

To obtain particular output results of the model, the "Integrated noise" function can be activated; by setting it, the Box-Jenkins formulation becomes:

$$y(t) = \frac{B_i(q)}{F_i(q)} u(t-nk) + \frac{C(q)}{D(q)} e(t) \frac{1}{1-q^{-1}} \tag{6.15}$$

where

$$\frac{1}{1-q^{-1}}$$

is the integrator of the noise channel.

6.4.3 Phases to identify the dynamic characteristics of the defective system

Steps to identify a model that highlights the presence of the defect in the steering system, using the polynomial model of the Box-Jenkins structure:

1. Selection of data in the time domain (input-output data were filtered in the frequency range 140 - 400 Hz, qualitatively identified range in signal processing in previous chapters).
2. Estimation of the coefficients of the Box-Jenkins polynomial model discrete in time, with testing the orders nb, nc, nd, nf, so as to obtain the best possible fit of the measured data with the estimated model, for each axis.
3. Obtaining the coefficients of the Box-Jenkins polynomial model as a continuous model in time by construction, for each axis, with the **d2c(sys)** function in Matlab.
4. Validation of the estimated model by comparing it with sequences of the measured signals, other than those used for estimation (with **compare** function in Matlab), on each of the three axes.
5. Extraction of dynamic models with a degree of freedom, excited by the presence of the defect (highlighted by their natural frequencies and damping rate).

6.4.4 Estimation of the parameters of the Box-Jenkins polynomial model discrete in time with the determination of the orders nb, nc, nd, nf, for each axis

The estimation of the parameters of the Box-Jenkins polynomial model corresponds to the recordings of the input-output acceleration signals of the Logan vehicle in motion, with a speed of 30km/h, on a route with bumps of the roadway. The input signal corresponds to the flawless system and the output signal corresponds to the defective system.

Box-Jenkins discrete time parameters for X-axis signals

bj55551 =
Discrete-time Polynomial with Noise Integration model: y(t) = [B(z)/F(z)]u(t) + [C(z)/D(z)(1-z^-1)]e(t)
B(z) = -0.4473 z^-1 - 0.538 z^-2 - 0.5606 z^-3 - 0.1744 z^-4 - 0.3137 z^-5
C(z) = 1 - 0.7171 z^-1 - 1.388 z^-2 + 1.137 z^-3 + 0.5828 z^-4 - 0.6149 z^-5
D(z) = 1 + 0.6766 z^-1 + 1.582 z^-2 + 0.521 z^-3 + 0.7201 z^-4 - 0.1186 z^-5
F(z) = 1 - 0.9098 z^-1 + 0.6768 z^-2 - 0.7827 z^-3 + 0.9377 z^-4 - 0.5475 z^-5
Sample time: 0.001 seconds
Parameterization:
Polynomial orders: nb=5 nc=5 nd=5 nf=5 nk=1
Number of free coefficients: 20
Model contains integration on noise channel.
Status:
Estimated using BJ on time domain data "Estimation".
Fit to estimation data: 79.43% (prediction focus)
FPE: 0.01225, MSE: 0.01166 (Final Prediction Error- FPE); (Mean Square Error- MSE)

Box-Jenkins discrete time parameters for Y-axis signals

bj55551 =
Discrete-time Polynomial with Noise Integration model: y(t) = [B(z)/F(z)]u(t) + [C(z)/D(z)(1-z^-1)]e(t)
B(z) = 0.4725 z^-1 - 0.07876 z^-2 + 0.6738 z^-3 - 0.05412 z^-4 + 0.2449 z^-5
C(z) = 1 - 0.2771 z^-1 - 0.6788 z^-2 - 0.03341 z^-3 - 0.3174 z^-4 + 0.3084 z^-5
D(z) = 1 + 0.4733 z^-1 + 1.569 z^-2 + 0.4527 z^-3 + 0.7938 z^-4 + 0.0002474 z^-5
F(z) = 1 - 0.5017 z^-1 + 1.209 z^-2 - 0.8057 z^-3 + 0.3752 z^-4 - 0.5473 z^-5
Sample time: 0.001 seconds
Parameterization:
Polynomial orders: nb=5 nc=5 nd=5 nf=5 nk=1
Number of free coefficients: 20
Model contains integration on noise channel.

Status:
Estimated using BJ on time domain data "Estimation".
Fit to estimation data: 71.9% (prediction focus)
FPE: 0.004317, MSE: 0.003995 (Final Prediction Error- FPE); (Mean Square Error- MSE)

Box-Jenkins discrete time parameters for Z-axis signals

bj55551 =
Discrete-time Polynomial with Noise Integration model: y(t) = [B(z)/F(z)]u(t) + [C(z)/D(z)(1-z^-1)]e(t)
B(z) = 0.01877 z^-1 - 0.02152 z^-2 + 0.03421 z^-3 - 0.003506 z^-4 + 0.0429 z^-5
C(z) = 1 - 0.1839 z^-1 - 0.6413 z^-2 + 0.03638 z^-3 - 0.3567 z^-4 + 0.1495 z^-5
D(z) = 1 + 0.4452 z^-1 + 1.466 z^-2 + 0.5483 z^-3 + 0.8819 z^-4 + 0.1143 z^-5
F(z) = 1 + 0.6161 z^-1 + 1.435 z^-2 + 0.6007 z^-3 + 0.9162 z^-4 + 0.1013 z^-5
Sample time: 0.001 seconds
Parameterization:
Polynomial orders: nb=5 nc=5 nd=5 nf=5 nk=1
Number of free coefficients: 20
Model contains integration on noise channel.
Status:
Estimated using BJ on time domain data "Estimation".
Fit to estimation data: 78.29% (prediction focus)
FPE: 0.004181, MSE: 0.003869 (Final Prediction Error- FPE); (Mean Square Error- MSE)

6.4.5 Development of the Box-Jenkins polynomial model continuously in time, with the determination of the orders nb, nc, nd, nf, for each axis

The Box-Jenkins model built continuously over time for X-axis signals

Sysc =
Continuous-time BJ model: y(t) = [B(s)/F(s)]u(t) + [C(s)/D(s)]e(t)
B(s) = -363.4 s^4 - 6.963e04 s^3 - 2.82e09 s^2 - 1.125e12 s - 4.281e15
C(s) = s^11 + 4016 s^10 + 1.663e07 s^9 + 4.248e10 s^8 + 7.683e13 s^7 + 1.306e17 s^6 + 1.096e20 s^5 + 1.014e23 s^4 + 4.167e25 s^3 + 1.788e28 s^2 + 2.875e30 s + 5.55e29
D(s) = s^11 + 2734 s^10 + 1.363e07 s^9 + 3.176e10 s^8 + 6.605e13 s^7 + 1.255e17 s^6 + 1.347e20 s^5 + 1.891e23 s^4 + 1.037e26 s^3 + 8.234e28 s^2 + 1.525e31 s + 1.195e19
F(s) = s^5 + 602.5 s^4 + 5.317e06 s^3 + 2.629e09 s^2 + 3.804e12 s + 7.883e14
Parameterization:
Polynomial orders: nb=6 nc=11 nd=11 nf=5 nk=0
Number of free coefficients: 32
Status:
Created by direct construction or transformation. Not estimated.

The Box-Jenkins model built continuously over time for Y-axis signals

Sysc =
Continuous-time BJ model: y(t) = [B(s)/F(s)]u(t) + [C(s)/D(s)]e(t)
B(s) = 575 s^4 + 3.746e05 s^3 + 2.586e09 s^2 + 8.724e11 s + 2.781e15
C(s) = s^7 + 1.781e04 s^6 + 1.069e08 s^5 + 2.097e11 s^4 + 4.486e14 s^3 + 3.857e17 s^2 + 2.064e20 s + 2.261e20
D(s) = s^7 + 1.638e04 s^6 + 8.479e07 s^5 + 1.149e11 s^4 + 4.688e14 s^3 + 1.769e17 s^2 + 6.031e20 s - 3.728e07
F(s) = s^5 + 602.8 s^4 + 5.924e06 s^3 + 2.098e09 s^2 + 7.776e12 s + 1.611e15
Parameterization:
Polynomial orders: nb=5 nc=7 nd=7 nf=5 nk=0
Number of free coefficients: 24
Status:
Created by direct construction or transformation. Not estimated.

The Box-Jenkins model built continuously over time for Z-axis signals

Sysc =
Continuous-time BJ model: y(t) = [B(s)/F(s)]u(t) + [C(s)/D(s)]e(t)
B(s) = 98.44 s^5 + 6.073e05 s^4 + 3.086e08 s^3 + 2.71e12 s^2 - 4.926e14 s + 1.674e18
C(s) = s^7 + 5581 s^6 + 2.539e07 s^5 + 4.574e10 s^4 + 9.024e13 s^3 + 6.722e16 s^2 + 4.493e19 s + 8.683e19
D(s) = s^7 + 4156 s^6 + 2.037e07 s^5 + 2.606e10 s^4 + 8.911e13 s^3 + 3.345e16 s^2 + 9.763e19 s - 9.29e07
F(s) = s^6 + 4434 s^5 + 2.124e07 s^4 + 2.899e10 s^3 + 9.878e13 s^2 + 3.987e16 s + 1.103e20
Parameterization:
Polynomial orders: nb=6 nc=7 nd=7 nf=6 nk=0
Number of free coefficients: 26
Status:
Created by direct construction or transformation. Not estimated.

6.4.6 Validation of the estimated Box Jenkins model, on each of the 3 axes

The validation of the estimated Box-Jenkins model could be done only for data in short time intervals and by increasing the orders of the model from 5 to 15 (input and output signals have considerable lengths). The overlap of the estimated-validated signals for the Box-Jenkins model of order 15 is different on the 3 axes and the percentage is in the range of 45-70%, and this is due to the general nonlinearities of the whole system with high noise level, including "chirp" type signals (figures 6.28 - 6.30). The lowest estimation-validation percentage (45%) corresponds to the signals on the X axis for which in the previous chapters there were large variations of accelerations.

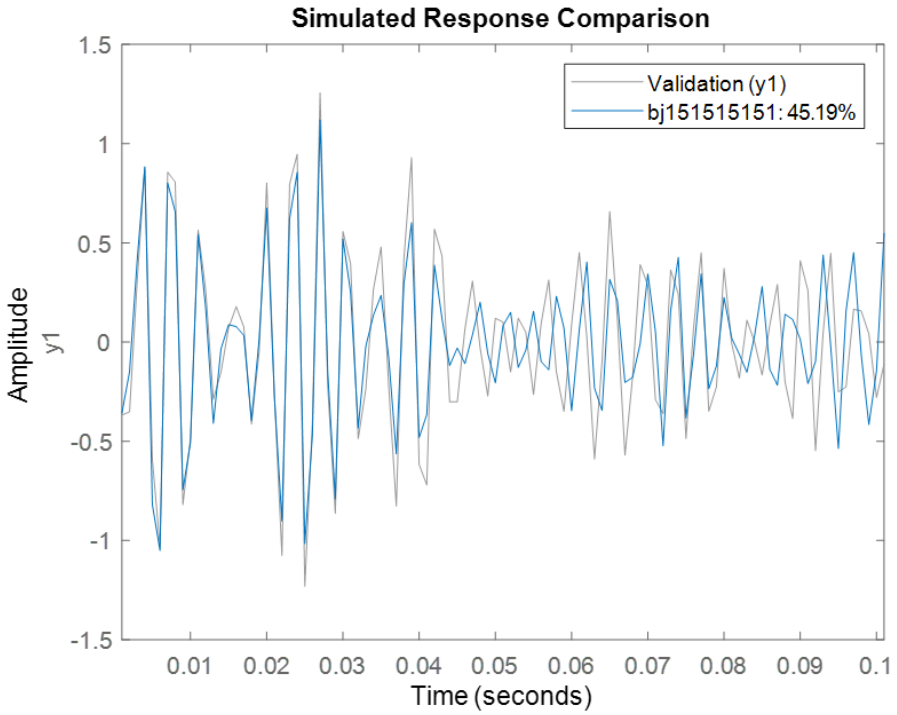

Figur 6. 10 Data validation for the X-axis input-output signal

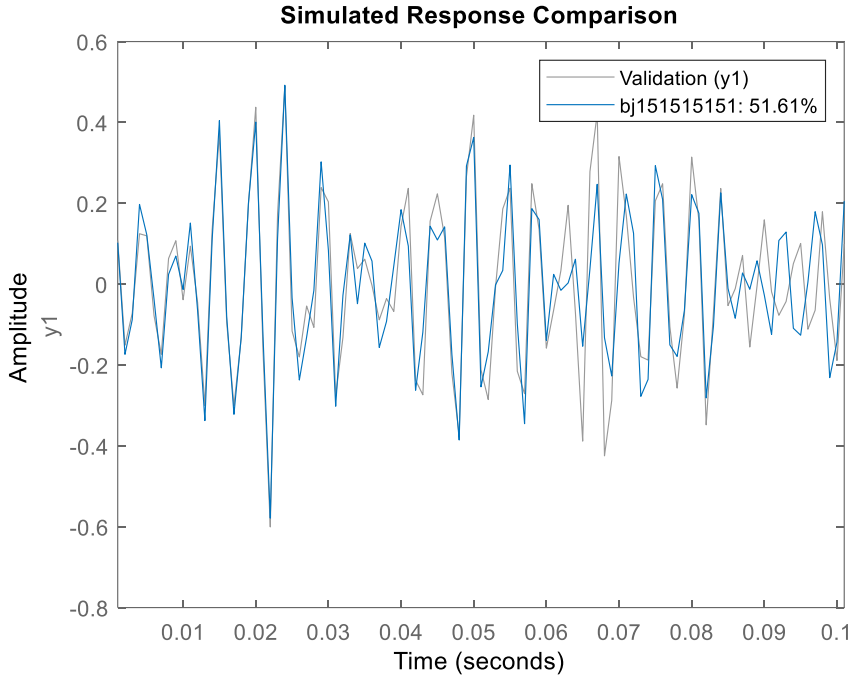

Figure 6. 11 Data validation for the Y-axis input-output signal

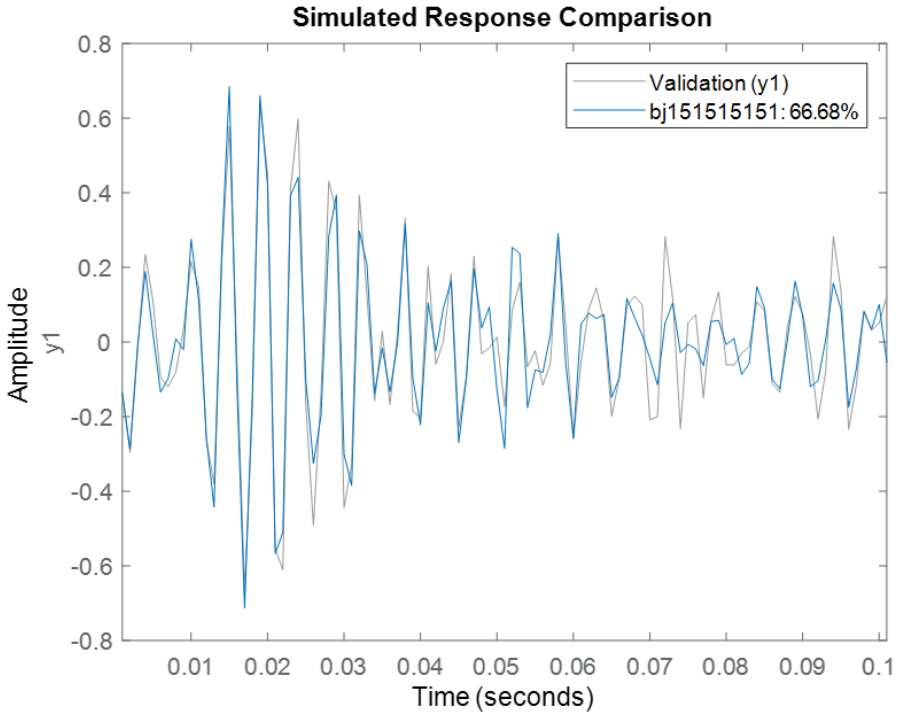

Figure 6. 12 Data validation for the Z-axis input-output signal

6.4.7 Extraction of dynamic models with a degree of freedom excited by the occurrence of the defect (highlighted by frequencies and damping rate)

Table 6. 2 Identification of modes excited by the presence of the defect on the X axis (Box-Jenkins model of order 5)

Mode	Natural frequencies [Hz]	Damping rate
1	141.03	0.17785
2	334.9	0.014385

Table 6. 3 Identification of modes excited by the presence of the defect on the Y axis (Box-Jenkins model of order 5)

Mode	Natural frequencies [Hz]	Damping rate
1	223.36	0.016777
2	312.52	0.087459

Table 6. 4 Identification of modes excited by the presence of the defect on the Z axis (Box-Jenkins model of order 5)

Mode	Natural frequencies [Hz]	Damping rate
1	208.91	0.034488
2	334.83	0.013025

6.4.8 The stability of the defective system in the states space

An identification model in the states space is a mathematical representation of a physical system characterized by input vectors, output vectors and state variables linked together by first-order differential equations. States variables define the values of the output variables. The model in the states space (modal variant) can represent a continuous or discrete model in time. The shape of the models in the states space in continuous representation in time is:

$$\dot{x}=Ax+Bu \quad (6.17)$$

$$y=Cx+Du \quad (6.18)$$

where **x**, **u** and **y** represent state variables, input and output vectors, while matrices **A, B, C, D** are states space matrices:

A - system matrix; B - input matrix; C - output matrix; D - control matrix from an external operator (in control systems - feedforward matrix).

The input-output data was filtered in the range of 140 Hz-400 Hz, the model in the state space in each direction of the measured data contains an input and an output. The number of states is 6 to ensure an adequate overlap (as much as possible) of the estimated data with the measured data.

6.4.9 Partial conclusions

The verification of the system estimated with the 5th order Box-Jenkins polynomial model showed that the estimated dynamic transfer function $G(s)=\frac{B(s)}{A(s)}$ can be considered adequate. The large variations of the measured accelerations, belonging to the input and output signals, are responsible for the increase of the noise level. The level of second-order accelerations (jerk) could quantify the presence of the defect in the analyzed spherical joint of the steering system. Considering that the estimated transfer function of the dynamic system $G(s)=\frac{B(s)}{A(s)}$ has been validated, using the Matlab **modalfit** function applied to the Box-Jenkins model estimated of order 5, natural frequencies and damping rate were obtained for the excited shock modes in each of the three axis.

6.5 The time-domain spectrogram processing and analysis. Accelerations jerk of the recorded signal

The comparative analysis of the vibration spectra, with or without defective tie rod end, analyzed the variations in time of the amplitudes of the vibration accelerations and the establishment of their correspondence with the appearance of multiple shocks in the spherical joint, for the 20 tests. Analysis of the data recorded in all 20 tests shows that the amplitudes of vibration accelerations recorded with existing defect are significantly higher, on all 3 axes, compared to those recorded in the same test conditions, but without existing defect.

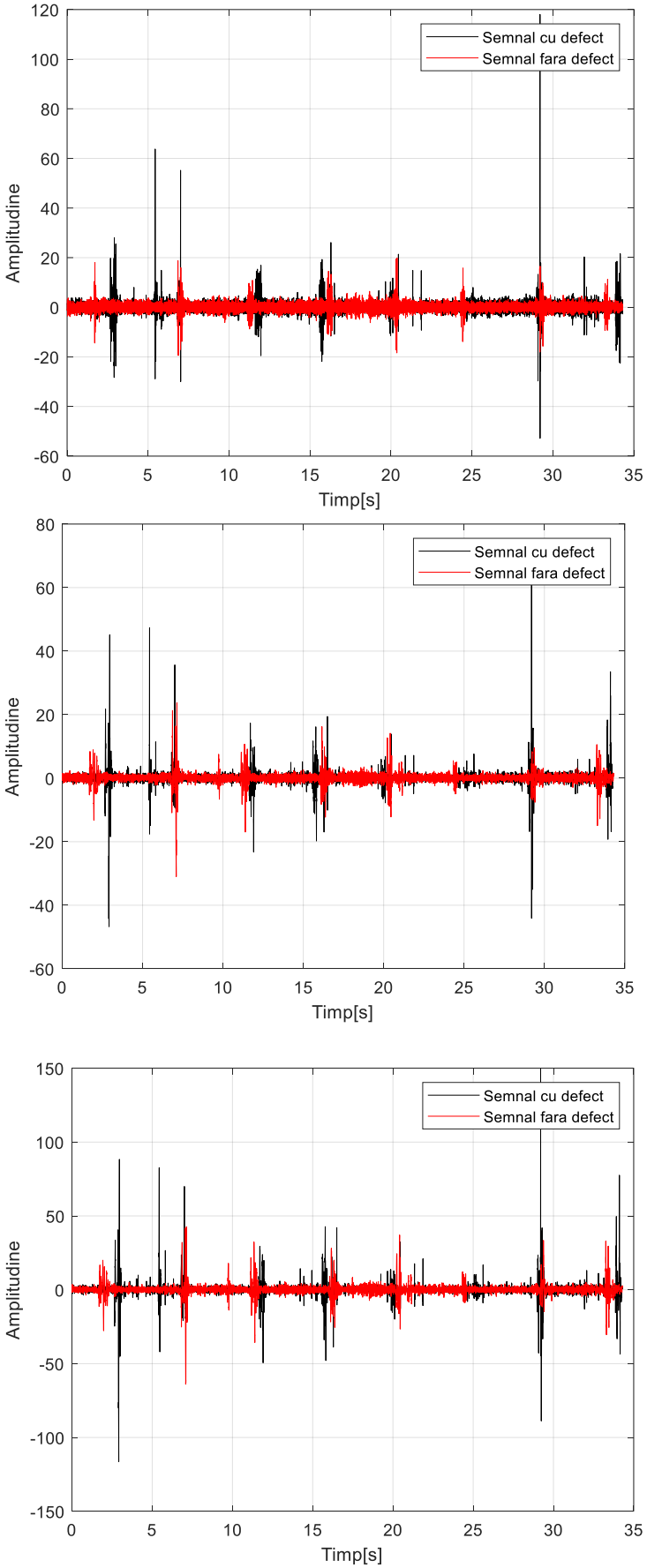

Figure 6. 13 The overlap of vibration spectra, test 3 (defective), test 4 (no defect): (a) on the OX axis; (b) on the OY axis; (c) on the OZ axis

The analysis of the overlap in time of the vibration spectra corresponding to the 10 pairs of tests performed, with and without defect, reveals significantly higher values of the amplitudes of the accelerations of the defective systems (graphs in black) compared to those of the systems without defect (graphs in red). The measure of imbalances in the steering system is revealed by the ratio between the maximum slope and the average slope of the accelerations of the recorded signals. The slope of the acceleration signal (second-order acceleration) is the variation of the acceleration over a period of time. In systems where shocks caused by the wear of the spherical joint of the tie rod end occur, the variation of acceleration in a short time has a significant value.

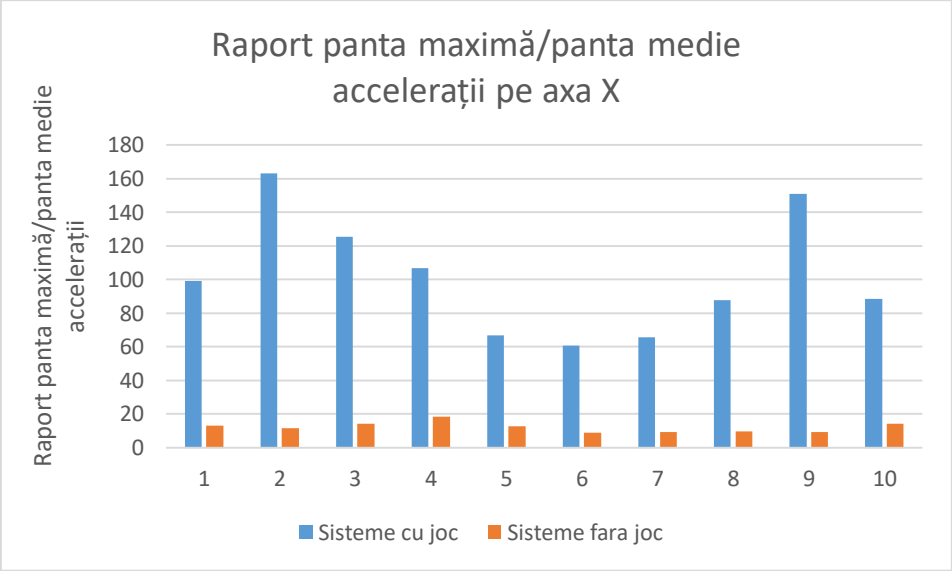

Figure 6. 14 The ratio between the maximum slope and the average slope of the accelerations on the OX axis for the 10 pairs of systems (with and without defect)

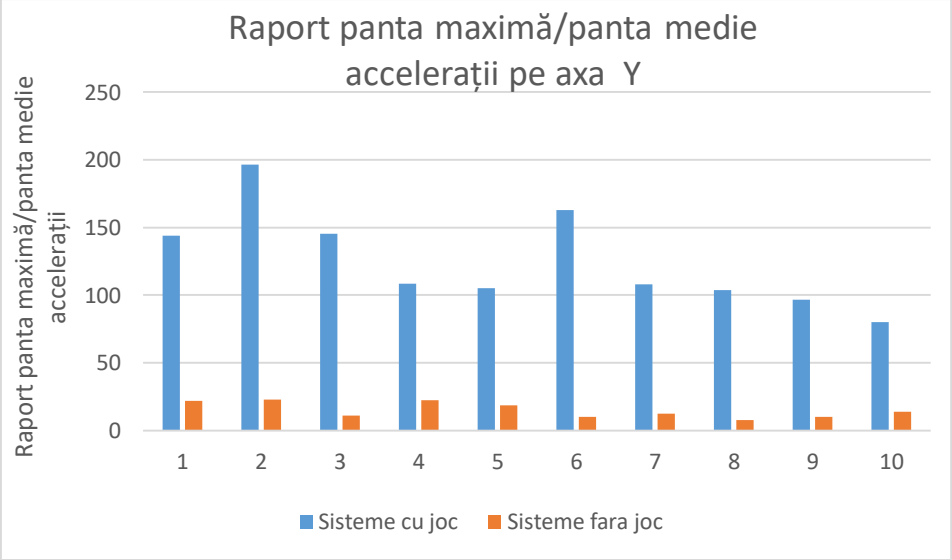

Figure 6. 15 The ratio between the maximum slope and the average slope of the accelerations on the OY axis for the 10 pairs of systems (with and without defect)

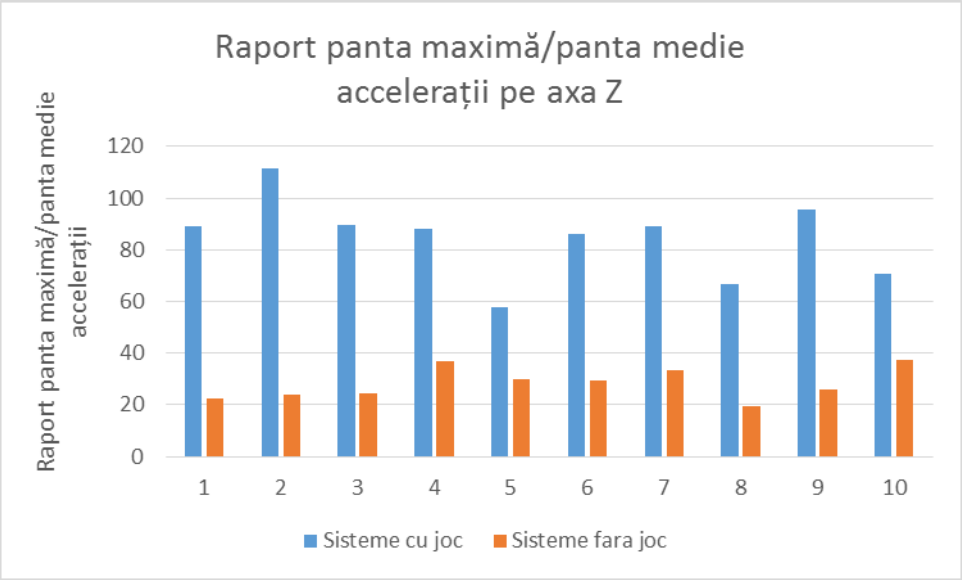

Figure 6. 16 The ratio between the maximum slope and the average slope of the accelerations on the OZ axis for the 10 pairs of systems (with and without defect)

From these comparisons it results that a limit ratio between the maximum slope and the average acceleration slope, with the value over 50 (figure 6.41, pairs 4 and 10), can indicate the appearance of the defect in the analyzed system. The value of 50 was determined considering that of all the tests performed, at pairs 4 and 10 on the OZ axis, for flawless systems, maximum values of the ratio between the maximum slope and the average slope of accelerations with values below 40 were recorded.

CHAPTER 7
GENERAL CONCLUSIONS OF THE DIAGNOSIS OF THE TECHNICAL CONDITION OF THE SPHERICAL JOINTS, PERSONAL CONTRIBUTIONS AND FUTURE RESEARCH DIRECTIONS

7.1 General conclusions

The wear of the spherical joints of the steering systems, defects encountered with high frequency in the vehicles operation, determine the change of the geometry of the steering wheels, leading to decreased stability and maneuverability, as well as premature tire wear. In case of separation of the spherical joint components (pivot case), the most serious effect may be the loss of vehicle control, by the sudden and independent turning of the wheel afferent to the tie rod end, generating a major risk of road accidents.

Although electronic control systems are being used more and more, on-board diagnostic systems are not implemented in vehicles to detect wear in the steering system joints.

Having as a starting point the faults symptoms that a driver perceives in driving (sounds, vibrations, abnormal shocks), the scientific research of the thesis aimed to diagnose wear of spherical joints produced at the tie rod-tie rod end assembly in the steering system, based on vibration analysis components.

The research results led to the conclusion that the response of the system to shock should be analyzed by identifying vibrations specific to the existence of the defect in frequency ranges and not by trying to identify single vibration frequencies, with well determined values, as in the case of stationary vibrations. Thus, by using the STFT procedure from Matlab, specific to non-stationary phenomena, a mark of the dynamic behavior of the system to shocks in the tie rod end was established, in the form of vertical bands highlighted in spectrograms, with high energy loads in certain frequency ranges.

The results highlighted the excitation of some frequencies corresponding to the own vibration modes of the analyzed ensemble, in the range of 100 - 400 Hz, frequencies identified also by using the finite element analysis program Ansys Workbench with the Modal module.

The mark of the system, resulting from the tests performed on the bench contains common elements with the dynamic mark established in the running, in the form of vertical bands of response to shocks in the joint, this mark being specific to the spectrograms of percussion music systems.

The response of the running system corresponds to both stationary vibrations (generated by engine operation and tire-driveway interaction), visible in the form of continuous horizontal waves, and non-stationary vibrations, in the form of vertical bands, with high energy loads in certain frequency ranges, corresponding to shocks.

The resulting data showed that the variation of kurtosis can be used to form a filter to select that part of the signal recorded corresponding to the shocks and, implicitly, the appearance of the defect, contributing to the improvement of the diagnostic capacity. Since the tie rod end wear is characterized by multiple shocks between the components, spectral kurtosis is useful to determinate the frequency bands dominated by the tie rod end error signals, containing excited fault frequencies.

In defective systems, the occurrence of shocks is determined by the wear of the spherical joint of the tie rod end, and their production generates significant variations of the registered accelerations, compared to the systems without defect. The analysis of the time

overlap of the vibration spectra corresponding to the 10 pairs of tests performed, with and without defect, revealed that the measure of imbalances in the steering system is given by the ratio between the maximum slope and the average slope of the recorded signal accelerations. Thus, based on the signals corresponding to the three axes, in the frequency range of 0-500 Hz, it was found that the ratio between the maximum slope and the average acceleration slope is very high in systems with defect, compared to those without defect. From these comparisons it resulted that the ratio between the maximum slope and the average acceleration slope, with the value above the limit (50 in the analyzed cases) may indicate the occurrence of the defect in the analyzed system.

The thesis highlights the possibility of monitoring the technical condition of the spherical joints of the steering system, analyzing the vibrations produced in different driving conditions of vehicles and, at the same time, opens the prospect of using intelligent devices to ensure early detection of these defects.

7.2 Personal contributions

In order to develop a method for diagnosing spherical joint wear of the steering system, starting from the symptoms perceived by an experienced driver (sounds, vibrations, abnormal shocks), the research in the doctoral thesis was based on a series of own contributions, as it follows:

1. Analysis of maintenance activities carried out within a large fleet of vehicles (over 400 vehicles). The analysis showed that the wear of the spherical joints is a type of defect that occurs with a high frequency in the steering systems of vehicles. Faults of this type occur at the tie rod, tie rod end and pivots. There are also many situations when vehicles are presented for periodic technical inspections, without their drivers having previously noticed the occurrence of defects in the spherical joints of the steering system. The consequences of these defects are the change in the geometry of the steering system, the loss of stability of the vehicle, both in corners and in straight running, difficulties in controlling the comanded trajectory, accelerated wear of tires or other components of the steering system and even risk of road accident. Early detection of such faults would play an important role in increasing road comfort and safety and in significantly reducing vehicle maintenance costs.
2. Analysis of the vehicle-driveway interaction, in order to detect the symptoms that attest the existence of wear of the steering system spherical joints. To perform the tests I selected a vehicle from the M1 category frequently encountered on Romanian roads, Dacia Logan model, manufactured in 2016. To perform vibration measurements I used a 4-channel digital recorder DA20-RION, with software data processing DA-20 VIEWER and CAT 78 WR - Version 4.018, as well as a triaxial accelerometer brand Brüel & Kjær, type 4321. For the calibration of the accelerometer I used the calibrator brand PCB 394C06, series 4147, having the calibration certificate no. 01.03-110 / 2019, issued by the National Institute of Metrology. I identified the sources of shocks and vibrations recorded on board the vehicle and established that the technical condition of the spherical joints of the steering system influences these shocks and vibrations. I based my research on the fact that driving over various pits and bumps, common in urban traffic, causes shocks in defective spherical joints. The shocks produced in the defective tie rod end excite natural vibrations modes of the tie rod - tie rod end assembly, the determination of the system response to these shocks being defining for the investigated diagnostic method.
3. Drawing the 3D model of the tie rod - tie rod end assembly from the steering system structure. Considering the complicated shape of this assembly, characterized by multiple curves and various section sizes, I tried modeling using a 3D scanner, the generated file being inappropriate, due to the fact that it could not be imported into the

Ansys program. Subsequently, using the Catia V5 program, I realized the 3D geometry of the analyzed assembly, the resulting model being exported as a file with the extension "step" in the finite element analysis program Ansys Workbench. I performed the discretization of the tie rod - tie rod end assembly model with solid elements, using the type of SOLID 187 element from the Ansys library, this being an element with 10 nodes and 3 degrees of freedom per node, representing the translations on the 3 coordinate axes. Thus, for the 3D geometry of the analyzed system, 66734 nodes and 37784 elements were defined.

4. Simulation of the shock response of the tie rod – tie rod end assembly using the Ansys Workbench finite element analysis program with the Modal module. I performed simulations of the free vibrations of the system depending on the size of the clearance in the spherical joint Teflon bushing/pivot head, the values of the clearance being included in the range measured on the analyzed samples. Through finite element modeling, I highlighted the influence of clearance size on the system fundamental frequency and the differences between the vibration of systems with and without defect, the most important of which is the "decoupling" of vibration modes when the defect occurs, justifying "shocks" in operation. Thus, I revealed the fact that the appearance of the wear and the increase of its value in the spherical joint pivot/teflon bushing leads to the decrease of the values of the natural frequencies, with predilection in case of the first natural frequency. I also revealed that the presence of wear in the spherical joint leads to a "decoupling" of the bending modes on the OX and OZ axes, in contrast to the first two modes in the flawless system, in which the bends along the two axes are coupled. The decoupling suggests an increase in the level of vibration in the bending planes.
5. Establishing the maximum load and wear directions. I designed the device for measuring the maximum clearance in the spherical joint, establishing a range of values of the maximum clearance for the batch of 10 used tie rod end analyzed. I sectioned the spherical joints and analyzed the mode of producing the wear of the spherical joint, establishing, at the same time, the directions of maximum stress and wear.
6. Experimental validation of the models made, by making experimental recordings on the test bench, to establish the response of the analyzed system to the shock. The vibration tests were performed on the test bench, the used devices being designed to apply shocks in the direction of producing maximum wear of the spherical joint of the tie rod end. I obtained the validation of the finite element modeling results, referring to the fundamental natural frequency and the other natural frequencies of the system. I established that the system response to shock must be analyzed by identifying vibrations specific to the existence of the defect in frequency ranges and not by trying to identify single vibration frequencies, with well-determined values, as in the case of stationary vibrations. Thus, by using STFT, I obtained a mark of the dynamic behavior of the system to shock, in the form of vertical bands, with high energy loads in certain frequency ranges, specific to the spectrograms of percussion music systems.
7. Experimental validation of the created models, by performing vibration recordings in driving, to establish the response of the analyzed system to shock, in different driving conditions and depending on the technical state of the spherical joint. I established that the driving system response corresponds to both stationary vibrations (generated by engine operation and tire-driveway interaction), visible in the form of continuous horizontal waves, and non-stationary vibrations, in the form of vertical bands, with high energy loads in certain frequency ranges, corresponding to shocks.
8. Highlighting the presence of defective in the spherical joint of the tie rod end using percussive components from the STFT spectrograms of accelerations, materialized by a multiple shock mark, in the form of vertical bands, in the range of 0-400 Hz.

9. Using the MATLAB functions, specific to the analysis of non-stationary signals: periodograms, STFT spectrograms highlighting the domains of variation of instantaneous frequencies, kurtograms to identify the position of highly non-stationary components in the vibration spectrum and optimal window length, useful in studying Spectral kurtosis. I performed the processing and presentation of the recorded signals for the systems with and without defect in the spherical joint, in a comparative manner, being obvious the delimitation of the harmonic components domain from that of the components corresponding to the multiple shock in the joint. The representation of Spectral kurtosis in the case of defective systems revealed components of the increasing variable frequency spectrum in the range of 150-350 Hz, with a maximum around 350 Hz, thus explaining the impossibility of applying a filter in this range, which would show a certain component (frequency) "controlled" by the size of the defective in the joint.
10. The use of second-order accelerations to highlight a limit value in the early diagnosis of wear in the spherical joint of the tie rod end. I analyzed the ratio between the maximum slope and the average slope of the accelerations of the recorded signals, as a measure of the imbalances in the steering system. I have established that in systems where shocks, favored by the wear of the spherical joint of the tie rod end occur, the variation of the acceleration in a short time has a significant value. Thus, I concluded that the value of the ratio between the maximum slope and the average acceleration slope, above a certain limit, may indicate the appearance of the defect.
11. Qualitative approaches to highlight the frequency ranges in which percussive components of signals appear, using MATLAB functions, as well as the possibility of early diagnosis of wear in the Teflon bushing/spherical joint pivot, using second-order acceleration, can be used in a methodology for analyzing highly non-stationary signals from shock operation.

7.3 Future research directions

The doctoral thesis opens new research perspectives in the diagnostics domain of the defective vehicle steering system during driving, in order to increase road comfort and safety and to reduce maintenance costs. For this reason, I propose the following research directions:

1. Analysis of the transmissibility of vibrations generated by the shocks produced in the defective spherical joints of the steering system, inside the passenger compartment of the vehicle.

2. Use of smart devices (mobile phones) equipped with an accelerometer to record vibration parameters in the passenger compartment, near the driver.

3. The use of neural networks to develop a methodology for analyzing highly non-stationary signals from shock operation, based on both the frequency ranges in which percussive components of the signals appear and the ratio between maximum and average slope of vibration accelerations.

4. Extension of the vibration analysis in order to diagnose other components of the vehicle, where shocks may occur in operation.

5. Development of a mobile diagnostic system to monitor the state parameters of the steering systems during the vehicle driving and to ensure the early detection of the occurrence of failures, in order to avoid the additional wear or road accidents.

SCIENTIFIC ACHIEVEMENTS

Publicații în reviste indexate SCOPUS

1. **Mihai Gingărașu**, Elena Mereuță, Valentin Amorțilă, Costel Humelnicu, THE INFLUENCE OF VEHICLE DIAGNOSIS ON REDUCING GAS EMISSIONS THAT AFFECTS THE EARTH'S CLIMATE SYSTEM, International Multidisciplinary Scientific GeoConference Surveying Geology and Mining Ecology Management, SGEM 2019, 19(4.1), pp. 1109-1116; ISBN 978-619-7408-83-6

2. **Mihai Gingărașu**, Elena Mereuță, Valentin Amorțilă, Costel Humelnicu, THE INFLUENCE OF VEHICLE STEERING SYSTEM MISSALIGNMENT ON THE ENVIRONMENT, International Multidisciplinary Scientific GeoConference Surveying Geology and Mining Ecology Management, SGEM 2019, 19(4.2), pp. 295-302; ISBN 978-619-7408-98-0

3. Valentin Amorțilă, Elena Mereuță, Costel Humelnicu, **Mihai Gingărașu**, DRIVER'S BIOMECHANICS INFLUENCE ON AIR POLLUTION, International Multidisciplinary Scientific GeoConference Surveying Geology and Mining Ecology Management, SGEM 2018, 18(4.3), pp. 251-258; ISBN 978-619-7408-70-6

4. Costel Humelnicu, Valentin Amorțilă, **Mihai Gingărașu**, Elena Mereuță, DAMAGING BY TRIBO-FATIGUE AND TEST RIG DESIGN, International Multidisciplinary Scientific GeoConference Surveying Geology and Mining Ecology Management, SGEM 2018, 18(4.3), pp. 235-242; ISBN 978-619-7408-70-6

5. Costel Humelnicu, Elena Mereuță, Valentin Amorțilă, **Mihai Gingărașu**, REDUCING THE AIR POLLUTION IMPACT OF THE RECYCLED AUTO VEHICLES, International Multidisciplinary Scientific GeoConference Surveying Geology and Mining Ecology Management, SGEM 2019, 19(4.1), pp. 1053-1060; ISBN 978-619-7408-83-6

6. Valentin Amorțilă, Elena Mereuță, Costel Humelnicu, **Mihai Gingărașu**, THE VIBRATION AND NOISE POLLUTION'S IMPACT ON THE DRIVER, International Multidisciplinary Scientific GeoConference Surveying Geology and Mining Ecology Management, SGEM 2019, 19(4.1), pp. 1143-1150; ISBN 978-619-7408-83-6

7. Valentin Amorțilă, Elena Mereuță,, Costel Humelnicu, **Mihai Gingărașu**, Monica Novetschi, CONTROVERSY ABOUT CAR POLLUTION: THE ELECTRIC VEHICLE OR THE CLASSIC VEHICLE?, International Multidisciplinary Scientific GeoConference Surveying Geology and Mining Ecology Management, SGEM 2019, 19(4.2), pp. 193-200; ISBN 978-619-7408-98-0

8. Costel Humelnicu, Elena Mereuță, Valentin Amorțilă, **Mihai Gingărașu**, FATIGUE POLYMERIC MATERIALS – AIR POLLUTION FACTOR, International Multidisciplinary Scientific GeoConference Surveying Geology and Mining Ecology Management, SGEM 2019, 19(4.2), pp. 221-228; ISBN 978-619-7408-98-0

Publicații în curs de indexare SCOPUS

1. **Mihai Gingărașu**, Elena Mereuță, Valentin Amortilă, Costel Humelnicu, Monica Novetschi, THE IMPORTANCE OF VEHICLE STEERING SYSTEM DIAGNOSIS IN REDUCING ENVIRONMENTAL IMPACT, International Multidisciplinary Scientific GeoConference Surveying Geology and Mining Ecology Management, SGEM 2020, (4.1), pp. 523-530; ISBN 978-619-7603-09-5

2. Costel Humelnicu, Elena Mereuță, Valentin Amorțilă, **Mihai Gingărașu**, Monica Novetschi, REDUCTION OF POLYMERIC WASTE BY APPLYING HEAT TREATMENTS DURING THE POLYMERIZATION PERIOD, International Multidisciplinary Scientific GeoConference Surveying Geology and Mining Ecology Management, SGEM 2020, (4.1), pp. 475-481; ISBN 978-619-7603-09-5

3. Monica Novetschi, Elena Mereuță, **Mihai Gingărașu**, Costel Humelnicu, Valentin Amorțilă, THE EFFECTS OF AUTO POLLUTION ON THE POPULATION, International Multidisciplinary Scientific GeoConference Surveying Geology and Mining Ecology Management, SGEM 2020, (4.1), pp. 499-506; ISBN 978-619-7603-09-5

Publicații în reviste indexate BDI

1. **Mihai Gingărașu**, Elena Mereuță, Valentin Amortilă, Costel Humelnicu, Monica Novetschi, WEAR OF SPHERICAL JOINTS OF THE VEHICLES STEERING SYSTEMS. VIBRATIONS AND THEIR ROLE IN DIAGNOSIS, Mechanical Testing and Diagnosis Scientific Journal, ”Dunărea de Jos” University, Galati, ISSN 2247 – 9635, 2020 (X), Volume 3, pp. 16-20

2. Costel Humelnicu, Valentin Amorțilă, Monica Novetschi, **Mihai Gingărașu,** ASPECTS REFERRING TO FATIGUE TESTING OF EPOXY POLYMERIC MATERIALS „Mechanical Testing and Diagnosis Scientific Journal”, ”Dunărea de Jos” University, Galati, ISSN 2247 – 9635, 2020 (X), Volume 3, pp. 21-25

3. Bogdan Gabriel Carp, **Mihai Gingăraşu**, Narcisa Cela Pînzariu, Serghei Palaş, Daniela Laura Buruiană, CONTRIBUTIONS TO INCREASING THE QUALITY OF URBAN LIFE THROUGH THE USE OF AN INTELLIGENT ROAD TRAFFIC MANAGEMENT SYSTEM, The Annals of “Dunărea de Jos” University of Galati Fascicle IX. Metallurgy and Materials Science No. 2 - 2017, ISSN 1453-083X, pp. 45-49

Lucrări prezentate la Conferințe Internaționale

1. Gabriel-Bogdan Carp, Narcisa Cela Pînzariu, Serghei Palaş, **Mihai Gingărașu**, Daniela Laura Buruiană, CONTRIBUTIONS TO INCREASING THE QUALITY OF URBAN LIFE THROUGH THE USE OF AN INTELLIGENT ROAD TRAFFIC MANAGEMENT SYSTEM, The Fourth International Conference New Trends In Environmental And Materials Engineering – TEME 2017, 25 - 27 octombrie 2017, Galați, România

2. **Mihai Gingăraşu**, Bogdan G. Carp, Elena Mereuţă, Daniela L. Buruiană, Marian Bordei, THEORETICAL RESEARCH ON THE DIAGNOSIS OF VEHICLE TECHNICAL CONDITION, The Sixth Edition of Scientific Conference Of Doctoral Schools SCDS-UDJG, 07 - 08 iunie 2018, Galați, România

3. Valentin Amorțilă, Elena Mereuță, Costel Humelnicu, **Mihai Gingărașu**, DRIVER'S BIOMECHANICS INFLUENCE ON AIR POLLUTION, International Multidisciplinary Scientific GeoConference Surveying Geology and Mining Ecology Management, Extended Scientific Sessions Vienna, SGEM 2018, 03 – 06 decembrie 2018, Viena, Austria

4. Costel Humelnicu, Valentin Amorțilă, **Mihai Gingărașu**, Elena Mereuță, DAMAGING BY TRIBO-FATIGUE AND TEST RIG DESIGN, International Multidisciplinary Scientific GeoConference Surveying Geology and Mining Ecology Management, Extended Scientific Sessions Vienna, SGEM 2018, 03 – 06 decembrie 2018, Viena, Austria

5. **Mihai Gingărașu**, Elena Mereuță, Valentin Amorțilă, Costel Humelnicu, Radu Bosoancă, DIAGNOSIS OF VEHICLE STEERING SYSTEMS USING VIBRATION ANALYSIS OF COMPONENT PARTS, The Seventh Edition of the Scientific Conference of the Doctoral Schools SCDS-UDJG, 13 – 14 iunie 2019, Galați, România

6. Valentin Amorțilă, Costel Humelnicu, **Mihai Gingărașu**, MASS-SPRING-DAMPER BIOMECHANICAL MODEL OF THE DRIVER, The Seventh Edition of the Scientific Conference of the Doctoral Schools SCDS-UDJG, 13 – 14 iunie 2019, Galați, România

7. Costel Humelnicu, Valentin Amorțilă, **Mihai Gingărașu**, Monica Novetschi, FATIGUE TESTING OF EPOXY RESIN BASED MATERIALS, Seventh Edition of the Scientific Conference of the Doctoral Schools SCDS-UDJG, 13 – 14 iunie 2019, Galați, România

8. **Mihai Gingărașu**, Elena Mereuță, Valentin Amorțilă, Costel Humelnicu, THE INFLUENCE OF VEHICLE DIAGNOSIS ON REDUCING GAS EMISSIONS THAT AFFECTS THE EARTH'S CLIMATE SYSTEM, International Multidisciplinary Scientific GeoConference Surveying Geology and Mining Ecology Management, SGEM 2019, 30 iunie – 06 iulie 2019, Albena, Bulgaria

9. Costel Humelnicu, Elena Mereuță**,** Valentin Amorțilă, **Mihai Gingărașu**, REDUCING THE AIR POLLUTION IMPACT OF THE RECYCLED AUTO VEHICLES, International Multidisciplinary Scientific GeoConference Surveying Geology and Mining Ecology Management, SGEM 2019, 30 iunie – 06 iulie 2019, Albena, Bulgaria

10. Valentin Amorțilă, Elena Mereuță, Costel Humelnicu, **Mihai Gingărașu**, THE VIBRATION AND NOISE POLLUTION'S IMPACT ON THE DRIVER, International Multidisciplinary Scientific GeoConference Surveying Geology and Mining Ecology Management, SGEM 2019, 30 iunie – 06 iulie 2019, Albena, Bulgaria

11. **Mihai Gingărașu**, Elena Mereuță, Valentin Amorțilă, Costel Humelnicu, THE INFLUENCE OF VEHICLE STEERING SYSTEM MISSALIGNMENT ON THE ENVIRONMENT, International Multidisciplinary Scientific GeoConference Surveying Geology and Mining Ecology Management, SGEM VIENNA GREEN 2019, 09 – 12 decembrie 2019, Viena, Austria

12. Costel Humelnicu, Elena Mereuță, Valentin Amorțilă, **Mihai Gingărașu**, FATIGUE POLYMERIC MATERIALS – AIR POLLUTION FACTOR, International Multidisciplinary Scientific GeoConference Surveying Geology and Mining Ecology Management, SGEM VIENNA GREEN 2019, 09 – 12 decembrie 2019, Viena, Austria

13. **Mihai Gingărașu**, Elena Mereuță, Valentin Amortilă, Costel Humelnicu, Monica Novetschi, THE WEAR OF THE SPHERICAL JOINTS OF THE VEHICLES STEERING SYSTEMS - VIBRATIONS AND THEIR ROLE IN DIAGNOSIS, The Eighth Edition of the Scientific Conference of the Doctoral Schools SCDS-UDJG, 18– 19 iunie 2020, Galați, România

14. Costel Humelnicu, Valentin Amorțilă, **Mihai Gingărașu**, Elena Mereuță, ASPECTS REFERRING TO FATIGUE TESTING OF EPOXY POLYMERIC MATERIALS, The Eighth Edition of the Scientific Conference of the Doctoral Schools SCDS-UDJG, 18– 19 iunie 2020, Galați, România

15. Monica Novetschi, Tarek Nazer, Costel Humelnicu, **Mihai Gingărașu**, Valentin Amortila, LOWER LIMB ANALYSIS WHEN THE CLUTCH PEDAL IS ACTUATED, The Eighth Edition of the Scientific Conference of the Doctoral Schools, SCDS-UDJG, 18– 19 iunie 2020, Galați, România

16. **Mihai Gingărașu**, Bogdan Gabriel Carp, SMART ROAD TRAFFIC MANAGEMENT SYSTEM, The Eighth Edition of the Scientific Conference of the Doctoral Schools SCDS-UDJG, 18– 19 iunie 2020, Galați, România

17. **Mihai Gingărașu**, Elena Mereuță, Valentin Amortilă, Costel Humelnicu, Monica Novetschi, THE IMPORTANCE OF VEHICLE STEERING SYSTEM DIAGNOSIS IN REDUCING ENVIRONMENTAL IMPACT, 20th International Multidisciplinary Scientific Conferences on Earth and Planetary Sciences SGEM 2020, virtual presentation, 16 – 25 august 2020, Albena, Bulgaria

18. Costel Humelnicu, Elena Mereuță, Valentin Amorțilă, **Mihai Gingărașu**, Monica Novetschi, REDUCTION OF POLYMERIC WASTE BY APPLYING HEAT TREATMENTS DURING THE POLYMERIZATION PERIOD, 20th International Multidisciplinary Scientific Conferences on Earth and Planetary Sciences SGEM 2020, virtual presentation, 16 – 25 august 2020, Albena, Bulgaria

Lucrări premiate la Conferințe Internaționale

1. **Mihai Gingăraşu**, Bogdan G. Carp, Elena Mereuţă, Daniela L. Buruiană, Marian Bordei, THEORETICAL RESEARCH ON THE DIAGNOSIS OF VEHICLE TECHNICAL CONDITION, The Sixth Edition of Scientific Conference Of Doctoral Schools SCDS-UDJG, 07 - 08 iunie 2018, Galați, România, Honourable Mention

2. Valentin Amorțilă, Costel Humelnicu, **Mihai Gingărașu**, MASS-SPRING-DAMPER BIOMECHANICAL MODEL OF THE DRIVER, The Seventh Edition of the Scientific Conference of the Doctoral Schools SCDS-UDJG, 13 – 14 iunie 2019, Galați, România, First Prize Award

3. **Mihai Gingărașu**, Elena Mereuță, Valentin Amortilă, Costel Humelnicu, Monica Novetschi, THE WEAR OF THE SPHERICAL JOINTS OF THE VEHICLES STEERING SYSTEMS - VIBRATIONS AND THEIR ROLE IN DIAGNOSIS, The Eighth Edition of the Scientific Conference of the Doctoral Schools SCDS-UDJG, 18– 19 iunie 2020, Galați, România, First Prize Award

SELECTIVE BIBLIOGRAPHY

[1] M. Gingarasu, E. Mereuta, V. Amortila, și C. Humelnicu, „The influence of vehicle diagnosis on reducing gas emissions that affects the Earth's climate system", *Int. Multidiscip. Sci. GeoConference SGEM*, vol. 19, nr. 4.1, pp. 1109–1115, 2019.

[2] M. Gingarasu, E. Mereuta, V. Amortila, C. Humelnicu, și M. Novetschi, „Wear of spherical joints of the vehicles steering systems. Vibrations and their role in diagnosis", *Mech. Test. Diagn.*, vol. 3, p. 5.

[3] M. Gingarasu, E. Mereuta, V. Amortila, și C. Humelnicu, „The influence of the vehicle steering system missalignment on the environment", *19th International Multidisciplinary Scientific GeoConference SGEM 2019*, vol. 19, nr. 4.2. STEF92 Technology, 51 Alexander Malinov blvd, Sofia, 1712, Bulgaria, pp. 295–302, dec. 09, 2019, doi: 10.5593/sgem2019V/4.2/S06.040.

[4] A. H. Falah, M. A. Alfares, și A. H. Elkholy, „Failure investigation of a tie rod end of an automobile steering system", *Eng. Fail. Anal.*, vol. 14, nr. 5, pp. 895–902, iul. 2007, doi: 10.1016/j.engfailanal.2006.11.045.

[5] S. K. Jha, „Characteristics and sources of noise and vibration and their control in motor cars", *J. Sound Vib.*, vol. 47, nr. 4, pp. 543–558, aug. 1976, doi: 10.1016/0022-460X(76)90881-6.

[6] S. He, T. Tang, E. Xu, M. Ye, și W. Zheng, „Vibration control analysis of vehicle steering system based on combination of finite-element analysis and modal testing":, *J. Vib. Control*, sep. 2019, doi: 10.1177/1077546319876798.

[7] M. Gingarasu, E. Mereuta, V. Amortila, C. Humelnicu, și M. Novetschi, „The importance of vehicle steering system diagnosis in reducing environmental impact", *Int. Multidiscip. Sci. GeoConference SGEM*, vol. 20, nr. 4.1, pp. 523–530, 2020.

[8] A. Reschka, M. Nolte, T. Stolte, J. Schlatow, R. Ernst, și M. Maurer, „Specifying a middleware for distributed embedded vehicle control systems", în *2014 IEEE International Conference on Vehicular Electronics and Safety*, dec. 2014, pp. 117–122, doi: 10.1109/ICVES.2014.7063734.

[9] A. H. Jamson, N. Merat, O. M. J. Carsten, și F. C. H. Lai, „Behavioural changes in drivers experiencing highly-automated vehicle control in varying traffic conditions", *Transp. Res. Part C Emerg. Technol.*, vol. 30, pp. 116–125, mai 2013, doi: 10.1016/j.trc.2013.02.008.

[10] J. Wang, L. Zhang, D. Zhang, și K. Li, „An Adaptive Longitudinal Driving Assistance System Based on Driver Characteristics", *IEEE Trans. Intell. Transp. Syst.*, vol. 14, nr. 1, pp. 1–12, mar. 2013, doi: 10.1109/TITS.2012.2205143.

[11] R. G. Herrtwich și G. Nöcker, „Cooperative Driving: Taking Telematics to the Next Level", în *Traffic and Granular Flow'01*, Berlin, Heidelberg, 2003, pp. 271–280, doi: 10.1007/978-3-662-10583-2_26.

[12] S. Damiani, E. Deregibus, și L. Andreone, „Driver-vehicle interfaces and interaction: Where are they going?", *Eur. Transp. Res. Rev.*, vol. 1, pp. 87–96, iul. 2009, doi: 10.1007/s12544-009-0009-2.

[13] H. Farah, H. N. Koutsopoulos, M. Saifuzzaman, R. Kölbl, S. Fuchs, și D. Bankosegger, „Evaluation of the effect of cooperative infrastructure-to-vehicle systems on driver behavior", *Transp. Res. Part C Emerg. Technol.*, vol. 21, nr. 1, pp. 42–56, apr. 2012, doi: 10.1016/j.trc.2011.08.006.

[14] W. Wachenfeld și H. Winner, „The Release of Autonomous Vehicles", în *Autonomous Driving: Technical, Legal and Social Aspects*, M. Maurer, J. C. Gerdes, B. Lenz, și H. Winner, Ed. Berlin, Heidelberg: Springer, 2016, pp. 425–449.

[15] „aide_day2_sp1_dve_leeds.pdf”. Data accesării: oct. 28, 2020. [Online]. Disponibil la: http://www.aide-eu.org/pdf/final_workshop/day2/sp1_session/aide_day2_sp1_dve_leeds.pdf.

[16] J. F. Coughlin, B. Reimer, și B. Mehler, „Driver wellness, safety & the development of an awarecar”, *AgeLab Mass Inst Technol Camb. MA*, 2009.

[17] K. Čulík, A. Kalašová, și S. Kubíková, „Simulation as an Instrument for Research of Driver-vehicle Interaction”, *MATEC Web Conf.*, vol. 134, p. 00008, 2017, doi: 10.1051/matecconf/201713400008.

[18] J. Wang, J. Wu, și Y. Li, „The Driving Safety Field Based on Driver–Vehicle–Road Interactions”, *IEEE Trans. Intell. Transp. Syst.*, vol. 16, nr. 4, pp. 2203–2214, aug. 2015, doi: 10.1109/TITS.2015.2401837.

[19] A. Capustiac, B. Hesse, D. Schramm, și D. Banabic, „A Human Centered Control Strategy for a Driving Simulator”, *Int. J. Mech. Mechatron. Eng. IJMME-IJENS*, vol. 11, pp. 45–52, feb. 2011.

[20] M. Zhang, C. Chen, T. Wo, T. Xie, M. Z. A. Bhuiyan, și X. Lin, „SafeDrive: Online Driving Anomaly Detection From Large-Scale Vehicle Data”, *IEEE Trans. Ind. Inform.*, vol. 13, nr. 4, pp. 2087–2096, aug. 2017, doi: 10.1109/TII.2017.2674661.

[21] D. Rimpas, A. Papadakis, și M. Samarakou, „OBD-II sensor diagnostics for monitoring vehicle operation and consumption”, *Energy Rep.*, vol. 6, pp. 55–63, feb. 2020, doi: 10.1016/j.egyr.2019.10.018.

[22] C. F. Tan, L. S. Wahidin, S. N. Khalil, N. Tamaldin, J. Hu, și G. W. M. Rauterberg, „The application of expert system: a review of research and applications”, vol. 11, nr. 4, p. 6, 2016.

[23] A. Adekunle, P. Ikubanni, și A. Olayinka, „An Expert System for Automobile Repairs and Maintenance”, vol. 16, pp. 41–56, dec. 2018.

[24] D. Piyabongkarn, R. Rajamani, J. A. Grogg, și J. Y. Lew, „Development and Experimental Evaluation of a Slip Angle Estimator for Vehicle Stability Control”, *IEEE Trans. Control Syst. Technol.*, vol. 17, nr. 1, pp. 78–88, ian. 2009, doi: 10.1109/TCST.2008.922503.

[25] A. C. Newberry, M. J. Griffin, și M. Dowson, „Driver perception of steering feel”, *Proc. Inst. Mech. Eng. Part J. Automob. Eng.*, vol. 221, nr. 4, pp. 405–415, apr. 2007, doi: 10.1243/09544070JAUTO415.

[26] T. D. Abilitare, „Universitatea Transilvania din Brașov”, p. 129.

[27] Y. Jiang, W. Deng, S. Zhang, S. Wang, Q. Zhao, și B. Litkouhi, „Studies on Influencing Factors of Driver Steering Torque Feedback”, SAE International, Warrendale, PA, SAE Technical Paper 2015-01–1498, apr. 2015. doi: 10.4271/2015-01-1498.

[28] B. George, A. T. Benny, A. John, A. Jose, și D. Francis, „Design and Fabrication of Steering and Bracking System for All Terrain Vehicle”, vol. 7, nr. 3, p. 12, 2016.

[29] T. D. Gillespie, „Fundamentals of Vehicle Dynamics”, *Warrendale PA Soc. Automot. Eng.*, p. 295, 1992.

[30] M. Abe, „Chapter 5 - Steering System and Vehicle Dynamics”, în *Vehicle Handling Dynamics (Second Edition)*, M. Abe, Ed. Butterworth-Heinemann, 2015, pp. 139–152.

[31] „wheelangles.jpg (548×450)”. https://www.design911.co.uk/blog/wp-content/uploads/2008/11/wheelangles.jpg (data accesării oct. 31, 2020).

[32] „Kingpin-Inc.gif (336×416)”. https://www.ictworkshopsolutions.com/ict2014/wp-content/uploads/2011/06/Kingpin-Inc.gif (data accesării oct. 31, 2020).

[33] „Condiţii privind starea tehnică – RNTR 1”, *Condiţii privind starea tehnică – RNTR 1*. http://www.rarom.ro/?page_id=631 (data accesării oct. 31, 2020).

[34] „Registrul Auto Român R.A.” http://www.rarom.ro/ (data accesării oct. 31, 2020).

[35] „ALTESCO-ESCON-detectoare-de-jocuri-2013.pdf”. Data accesării: dec. 04, 2020. [Online]. Disponibil la: http://www.totaltrading.ro/assets/images/ALTESCO-ESCON-detectoare-de-jocuri-2013.pdf.

[36] „Desktop NVH Simulator - Driving Simulator | Brüel & Kjær”. https://www.bksv.com/en/products/Analysis-software/vehicle-noise-vibration-and-harshness-software/vehicle-nvh-simulators-8601 (data accesării oct. 31, 2020).

[37] „Controlul vibratiilor Si zgomotului Dragan Barbu”, *pdfslide.tips*. https://pdfslide.tips/documents/controlul-vibratiilor-si-zgomotului-dragan-barbu.html (data accesării oct. 31, 2020).

[38] R. Burdzik, Ł. Konieczny, și T. Figlus, „Concept of On-Board Comfort Vibration Monitoring System for Vehicles”, în *Activities of Transport Telematics*, Berlin, Heidelberg, 2013, pp. 418–425, doi: 10.1007/978-3-642-41647-7_51.

[39] M. F. Mitroi, „29-91 Considerații privind influența vibrațiilor aleatoare induse de vehicule și calea de rulare organismului uman – Știință și Inginerie”. http://stiintasiinginerie.ro/29-91-consideratii-privind-influenta-vibratiilor-aleatoare-induse-de-vehicule-si-calea-de-rulare-organismului-uman/ (data accesării oct. 31, 2020).

[40] Deulgaonkar V.R, Kallurkar S.P, și Mattani A.G, *Review and Diagnostics of noise and vibrations in automobiles, International Journal of Modern Engineering Research (IJMER), Vol.1, Issue2, pp 242-246, ISSN: 2249-6645*. .

[41] P. M. Harikrishnan și V. P. Gopi, „Vehicle Vibration Signal Processing for Road Surface Monitoring”, *IEEE Sens. J.*, vol. 17, nr. 16, pp. 5192–5197, aug. 2017, doi: 10.1109/JSEN.2017.2719865.

[42] A. H. Falah, M. A. Alfares, și A. H. Elkholy, „Failure investigation of a tie rod end of an automobile steering system”, *Eng. Fail. Anal.*, vol. 14, nr. 5, pp. 895–902, iul. 2007, doi: 10.1016/j.engfailanal.2006.11.045.

[43] „Somic Ishikawa Inc”. http://www.somic.co.jp/ (data accesării iul. 05, 2020).

[44] A. H. Hauglid, „Nonlinear Mechanical Vibrations: The Effect of Gaps”, 2018, Data accesării: oct. 31, 2020. [Online]. Disponibil la: https://ntnuopen.ntnu.no/ntnu-xmlui/handle/11250/2562811.

[45] G. Yu și J.-J. Slotine, „Audio classification from time-frequency texture”, în *2009 IEEE International Conference on Acoustics, Speech and Signal Processing*, Taipei, Taiwan, apr. 2009, pp. 1677–1680, doi: 10.1109/ICASSP.2009.4959924.

[46] B. Thoshkahna și K. R. Ramakrishnan, „A postprocessing technique for improved harmonic / percussion separation for polyphonic music”, *12th Int. Conf. Music Inf. Retr. ISMIR11 Miami USA Oct. 2011*, p. 6, 2011.

[47] „L_Percussion.pdf”. Data accesării: iul. 13, 2020. [Online]. Disponibil la: http://astro.pas.rochester.edu/~aquillen/phy103/Lectures/L_Percussion.pdf.

[48] „Google Maps”, *Google Maps*. https://www.google.ro/maps/@45.4343201,28.0350193,3a,75y,184.22h,56.8t/data=!3m6!1e1!3m4!1s8ruRsWyKTNHWLXxOQWRMbA!2e0!7i13312!8i6656 (data accesării nov. 30, 2020).

[49] P. Sun, Y. Liao, și J. Lin, „The Shock Pulse Index and Its Application in the Fault Diagnosis of Rolling Element Bearings”, *Sensors*, vol. 17, nr. 3, Art. nr. 3, mar. 2017, doi: 10.3390/s17030535.

[50] G. M. Nita, „Spectral Kurtosis statistics of transient signals”, *Mon. Not. R. Astron. Soc.*, vol. 458, nr. 3, pp. 2530–2540, mai 2016, doi: 10.1093/mnras/stw550.

[51] N. Sawalhi și R. B. Randall, „The Application of Spectral Kurtosis to Bearing Diagnostics”, *Proc. Acoust. 2004 3-5 Novemb. 2004 Gold Coast Aust.*, pp. 393–398, 2004.

[52] J. J. G. De la Rosa, J. M. Sierra-Fernández, J. C. Palomares-Salas, A. Agüera-Pérez, și Á. J. Montero, „An Application of Spectral Kurtosis to Separate Hybrid Power Quality Events”, *Energies*, vol. 8, nr. 9, Art. nr. 9, sep. 2015, doi: 10.3390/en8099777.

[53] Y. Li, W. Song, F. Wu, E. Zio, și Y. Zhang, „Spectral Kurtosis of Choi–Williams Distribution and Hidden Markov Model for Gearbox Fault Diagnosis”, *Symmetry*, vol. 12, nr. 2, Art. nr. 2, feb. 2020, doi: 10.3390/sym12020285.

[54] Y. Jin, Z. Chen, L. Fan, și C. Zhao, „Spectral Kurtosis–Based Method for Weak Target Detection in Sea Clutter by Microwave Coherent Radar”, *J. Atmospheric Ocean. Technol.*, vol. 32, nr. 2, pp. 310–317, feb. 2015, doi: 10.1175/JTECH-D-13-00108.1.

[55] „Prelegerea_VI.pdf”. Data accesării: iul. 15, 2020. [Online]. Disponibil la: http://www.tex.tuiasi.ro/biblioteca/carti/CURSURI/Conf.%20dr.%20mat.%20Valeria%20Slabu/cursuri-Statistica/PRELEGEREA_VI.pdf.

[56] V. Vrabie, P. Granjon, și C. Serviere, „Spectral kurtosis: from definition to application”, în *6th IEEE International Workshop on Nonlinear Signal and Image Processing (NSIP 2003)*, Grado-Trieste, Italy, 2003, p. xx, Data accesării: nov. 28, 2020. [Online]. Disponibil la: https://hal.archives-ouvertes.fr/hal-00021302.

[57] „Spectral kurtosis from signal or spectrogram - MATLAB pkurtosis - MathWorks Switzerland”. https://ch.mathworks.com/help/signal/ref/pkurtosis.html (data accesării iul. 15, 2020).

[58] W. L. Young, „The Box-Jenkins approach to time series analysis and forecasting : principles and applications”, *RAIRO - Oper. Res. - Rech. Opérationnelle*, vol. 11, nr. 2, pp. 129–143, 1977.

[59] D. Piga, V. Breschi, și A. Bemporad, „Estimation of jump Box–Jenkins models”, *Automatica*, vol. 120, p. 109126, oct. 2020, doi: 10.1016/j.automatica.2020.109126.